Energy Intensity and Greenhouse Gas Emissions from Crude Oil Production in the Bakken Formation: Input Data and Analysis Methods

Adam R. Brandt[1], Tim Yeskoo[2], Scott McNally[3], Kourosh Vafi[1], Hao Cai[4], Michael Q. Wang[4]

[1]Department of Energy Resources Engineering, Stanford University
[2]Department of Civil and Environmental Engineering, Stanford University
[3]Kennedy School of Government, Harvard University
[4]Systems Assessment Group, Energy Systems Division, Argonne National Laboratory

September 2015

Prepared for Systems Assessment Group

Energy Systems Division
Argonne National Laboratory

TABLE OF CONTENTS

LIST OF FIGURES

LIST OF FIGURES (CONT.)

LIST OF TABLES

LIST OF TABLES (CONT.)

ACRONYMS AND ABBREVIATIONS

API	American Petroleum Institute
bbl/day	barrels of oil per day
DMR	North Dakota Department of Mineral Resources
DTD	drilling total depth
EDF	Environmental Defense Fund
EUR	estimated ultimate recovery
GHG	greenhouse gas
GOR	gas-oil ratio
gpm	gallons per minute
HD	Hyperbolic Decline
IPT	initial production test
LHV	lower heating value
NDPA	North Dakota Pipeline Authority
NGL	natural gas liquid
OPGEE	Oil Production Greenhouse Gas Emissions Estimator
PI	productivity index
ROP	rate of penetration
SE	Stretched Exponential
TVD	true vertical depth
WOR	water-oil ratio

Energy Intensity and Greenhouse Gas Emissions from Crude Oil Production in the Bakken Formation: Input Data and Analysis Methods

Adam R. Brandt, Tim Yeskoo, Scott McNally, Kourosh Vafi, Hao Cai, Michael Q. Wang

ABSTRACT

The Bakken formation has contributed to the rapid increase in U.S. oil production over the last five years. Crude oil is produced from the Bakken formation using high-volume hydraulic fracturing techniques to greatly increase formation permeability. In this study, we estimate the energy intensity and emissions associated with Bakken crude oil production. Using data from 7271 wells, collected from the years 2006 to 2013, we utilize the Oil Production Greenhouse Gas Emissions Estimator model, with some supplementary calculations performed using decline curve fitting models and a recently developed drilling and fracturing energy consumption model.

The total energy consumption is of order 1.7% of the energy content of produced crude. Production-weighted average energy intensities for natural gas, diesel, and electricity consumption are approximately 13,200, 1,800, and 50 Btu/mmBtu respectively, computed on a monthly operating basis. Amortized drilling and fracturing diesel energy use adds a production-weighted mean intensity of ~1900 Btu/mmBtu. Total consumption (production-weighted mean) is therefore 16,900 Btu/mmBtu. Fugitive emissions are not modeled on a per-well basis because of a lack of well-specific data, but for a "typical" Bakken well, they are estimated at 35 scf/bbl, or some 3% of the median Bakken gas produced. Depending on the year, between 5% and 15% of the equivalent energy content of the crude oil produced in the Bakken is flared as wasted natural gas. In 2013, the production-weighted average flaring rate was ~500 scf/bbl for wells that flared at least some gas. This rate equals about 14% of the energy content of the produced crude oil, or 140,000 Btu/mmBtu.

Bakken wells produce a significant amount of co-product energy along with the reported crude oil production. In 2013, natural gas exports (after deducting on-site natural gas use and gas flaring) equaled some 50,000 Btu/mmBtu crude oil, while export of natural gas liquids was approximately 140,000 Btu/mmBtu crude oil.

1 INTRODUCTION

In December 2014, the State of North Dakota produced over 1.2 million barrels of oil per day (bbl/day) [1], predominantly from the Bakken formation. Owing to the introduction of horizontal drilling with high-volume hydraulic fracturing, production of oil in the Bakken has increased rapidly from under 100,000 bbl/day in 2005.

The Bakken formation extends over parts of North Dakota, Montana, South Dakota, Saskatchewan and Manitoba. Most development to date has focused on the core Bakken region of northwestern North Dakota. The core Bakken formation lies 10,000 to 11,000 feet deep, although the edges of the basin are much shallower. Rapid development of the basin now means that thousands of wells are drilled per year in the Bakken (e.g., ~2600 new well "spuds" in 2014) [2].

Little information exists about the greenhouse gas (GHG) impacts of oil production in the Bakken. A small number of modeling studies have examined Bakken crude oil. Some work for the California Air Resources Board has examined the GHG intensity of Bakken crude oil, finding emissions on the order of 10.2 gCO2eq./MJ of crude oil produced [3]. Work by the United States Department of State has suggested that extraction of Bakken crude oil may be 20% more GHG-intensive compared to the National Energy Technology Laboratory U.S. crude oil baseline, which includes imported crude oil [4]. This figure was based in part on earlier work by the California Air Resources Board. An industry study prepared by IHS CERA, using the Oil Production Greenhouse Gas Emissions Estimator (OPGEE) model of Stanford University, found that Bakken crude oil emits 9.1 gCO2eq./MJ of crude oil produced [5, 6].

Empirical scientific studies in the Bakken region are rare. Some remote sensing studies have found elevated methane emissions over the region encompassing the Bakken formation [7], while others have found no such signal [8]. Recent airborne sampling work suggests that non-sputtering flares in the Bakken have high methane destruction efficiencies of above 99% [9].

In order to improve the understanding of Bakken crude oil GHG intensity, this paper outlines methods to collect data and model the energy intensity of Bakken crude oil production. The life-cycle GHG intensity of the Bakken formation crudes is then computed using the OPGEE model. Because horizontal drilling and hydraulic fracturing of the Bakken constitute a new method of resource development, we perform significant extensions of the OPGEE model to estimate the energy requirements of drilling and fracturing these wells.

This report is organized as follows: First, we outline the methods for collecting and analyzing information about wells in the Bakken formation. We begin with an overview of the process, then discuss data collection and processing, and then discuss model developments required to estimate energy use. Next, we illustrate and discuss results for the energy intensity of crude oil production in the Bakken. We conclude with needs for further work, remaining uncertainties, and an overall assessment of the impacts of crude production from the Bakken formation.

2 METHODS

This section outlines the methods of data collection and analysis, with extensive discussion of methods for gathering and cleaning data to prepare them for use in the OPGEE model.

2.1 Methods Overview

Data were collected from a variety of sources, with an emphasis on public datasets produced by the State of North Dakota. These data come from the North Dakota Department of Mineral Resources (henceforth DMR). These data were collected on a monthly basis for all relevant wells in the Bakken. Cleaning and compilation of the data resulted in the removal of some data points from the sample set, resulting in a final dataset of 7271 wells, nearly all related to Bakken production (see below for description of cleaning method). Monthly operating data were collected from January 2005 to May 2014. Because we only have four months of data for 2014 in our dataset, we end the analysis with the last available complete year (2013). Because few wells existed in 2005 and results from those months are highly erratic, we begin all time-series analyses with January 2006.

Other technical data specific to Bakken drilling and production were collected from the technical literature, with an emphasis on Society of Petroleum Engineers data where possible. These data were incorporated into the OPGEE model. Each well/month combination was assessed separately, allowing study of the distribution of emissions within a given time period across wells, or across the same well over time.

2.2 Data Collection

Data were collected from a variety of sources, and included well-level property data; well-level production data; and a variety of basin-wide data on drilling efficiency, production and processing practices, and land use impacts.

2.2.1 Well-Level Data

Detailed data were purchased from DMR [1, 2, 10, 11]. The data were delivered in July 2014 in .csv form. We purchased all data available in DMR datasets, which were delivered in four files: wellmaster.csv, all_prod.csv, geoprodtest.csv, and geostimulations.csv, totaling approximately 400 MB of raw data. The largest dataset was the all_prod dataset, which contained over 220,000 well-month observations that were relevant to this study.
DMR datasets can be summarized as follows:

1. *wellmaster.csv*: This table contains basic information about each well, such as the well name, company, location, status, and type. The wellmaster file also contains

multiple records for each well describing casing types, depths [ft], and diameters [in.], as well as drilling total depths [ft] and true vertical depths [ft]. Analysis of the well geometries and casing design is discussed below. The entries in wellmaster.csv are detailed in Table 1.

2. all_prod.csv: The production dataset is a monthly dataset containing the following information for each well in North Dakota: oil produced [bbl/month], gas produced [mcf/month], gas used on site [mcf/month], gas flared [mcf/month], gas vented [mcf/month], oil runs [bbl/month], and days of production [days]. Oil runs represent the oil volume sent to market from on-site storage, which can be less than or greater than the oil produced in a particular month. The pool name that the well is completed in (perhaps more accurately described as a well characteristic, as above) is also found in this table. The entries in *all_prod.csv* are detailed in Table 2.
3. *geoprodtest.csv*: This table contains dozens of pieces of information about various tests conducted in wells at various times and depths. Information of interest for this study includes bottom hole pressure tests [psi], gas analyses [mol fraction], gas-oil ratio (GOR) tests [scf/bbl], initial production tests [flow rate in bbl per day, pressure in psi] production tests, and oil analyses [deg. API]. We do not include a tabular listing of data from this dataset because of the large number of data columns (most of which are not used in this study) and unclear definitions of some columns.
4. geostim.csv: The geostim table contains information about specific stimulations performed on each well. The main fields include the location in the well where the well was stimulated, the volume of fracturing fluid used, the total weight of proppant, the pressure at which the fluid was injected, and the number of stages. This file is perhaps the least organized of all the files provided by DMR, with the "Comments" field containing various data that would more accurately be reported in other fields. The entries in *geostim.csv* are detailed in Table 3.
5. *wellindex.xlsx*: This is a supplemental table available on the DMR website that contains additional information, such as well geometry (e.g., horizontal and vertical), spud date, and location (latitude, longitude, township, range).

The four tables in flat file (.csv) format were imported into a SQL database so that the information could be readily cleaned, organized, and queried for analysis. The common key for connecting information from multiple tables for a single well was the Wl_Permit identifier allocated by the State of North Dakota. This is a unique identifier akin to the well API number.

Table 1. Data fields in the "wellmaster" dataset [2]

Column Header	Definition
API_WellNo	Well number, API (unique) [-]
Wl_Permit	DMR well permit number (unique, North Dakota-specific) [-]
Well_Nm	Well name [-]
CoName	Company name [-]
Well_Typ	Type of well (oil and gas, water injection, etc.) [-]

Table 1. (Cont.)

Column Header	Definition
Wl_Status	Well status (operational, shut in, abandoned, dry) [-]
Wh_Lat	Wellhead latitude [deg.]
Wh_Long	Wellhead longitude [deg.]
DTD	Drilling total depth (length of bore, including inclined and horizontal sections) [ft]
TVD	True vertical depth (depth of deepest part of well) [ft]
Typ_Pipe	Type of casing in listed casing section [-]
Bot	Bottom of casing section [ft]
Dia	Diameter of casing (API standard in most cases) [in.]
Top_	Top of casing section [ft]
WellConfidential	Is well confidential? [logical]

Table 2. Data fields in the "all_prod" dataset [1]

Column Header	Definition
API_WELLNO	Well number, API (unique) [-]
Wl_Permit	DMR well permit number (unique, North Dakota-specific) [-]
Well_Nm	Well name [-]
CoName	Company name [-]
RPT_DATE	Reporting date for production data [day]
WELL_TYP	Well type (oil and gas, water injection) [-]
MCF_GAS	Thousand cubic feet of gas [mcf]
MCF_LEASE	Thousand cubic feet of gas combusted on site ("lease use") in boilers and engines [mcf]
FLARED	Thousand cubic feet of gas flared [mcf]
VENTED	Thousand cubic feet of gas vented [mcf]
MCF_SOLD	Thousand cubic feet of gas sold [mcf]
BBLS_OIL_COND	Barrels of oil and condensate produced [bbl]
DAYS_PROD	Days of production in the month [days]
OIL_RUNS	Oil and condensate sold offsite [bbl]
BBLS_WTR	Barrels of water produced [bbl]
Pool_Nm	Name of pool [-]

Table 3. Data fields in the "geostim" dataset [11]

Column Header	Definition
API_WellNo	Well number, API (unique) [-]
Wl_Permit	DMR well permit number (unique, North Dakota-specific) [-]
Well_Nm	Well name [-]
Dt_Treat	Date of stimulation or treatment [day]
Top_	Well depth at top of treatment [ft]
Bot	Well depth at bottom of treatment [ft]
Stim_Hole	Type of casing in stimulated area (open-hole or cased) [-]
OH_Top	Depth at top of open-hole section [ft]

Table 3. (Cont.)

Column Header	Definition
OH_Base	Depth at bottom of open-hole section [ft]
Frac_Acid	Fracturing acid used (e.g., HCl; also includes "sand" for many modern wells.) [-]
Units	Unit of fluid injection reported (e.g., gallons, barrels) [-]
Vol	Volume of fracturing fluid injected [varies]
Lbs_Prop	Pounds of proppant injected [lb]
Acid_Con	Unknown (likely acid concentration)
MTPress	Fracturing pressure applied [psi]
Cmmnt	Comment [-]
Stages	Fracturing stages [-]
PoolNo	Number of pool [-]
MTRate_N	Unknown (likely rate of injection)
Pool_Nm	Name of pool [-]
WellConfidential	Is well confidential? [logical]

2.2.2 Creating a Representative Set of Bakken Wells

First, the data were cleaned to include only wells in the Bakken formation. The criteria used for inclusion were as follows:

1. The pool name field in the production dataset includes the word ‘Bakken,’ alone or in combination (‘Bakken/Three Forks,’ ‘Lodgepole/Bakken’).
2. The well type field in the wellmaster table is ‘OG,’ indicating an oil and gas well. The following well types are excluded: ‘AGD’ = acid gas disposal; ‘AI’ = air injection; ‘CBM’ = coal bed methane; ‘DF’ = dump flood injector; ‘DFP’ = dump flood injector/producer; ‘GASC’ = gas condensate; ‘GASD’ = dry gas; ‘GASN’ = nitrogen gas well; ‘GI’ = gas injection; ‘GS’ = gas storage; ‘INJP’ = injector/producer; ‘ST’ = stratigraphic test; ‘SWD’ = salt water disposal; ‘WI’ = water injection; ‘WS’ = water source.
3. The well status in the wellmaster table is ‘A’ (active), ‘PA’ (previously active), ‘IA’ (inactive), ‘AB’ (abandoned), ‘TA’ (temporarily abandoned), or ‘PA’ (plugged and abandoned). We include abandoned wells so as to avoid removing wells that were producing for a portion of the time period of interest but were abandoned at a later time. Other well statuses, such as ‘DRY’ (dry), ‘DRL’ (drilling), ‘PNC’ (permit now cancelled), ‘EXP’ (expired permit), and ‘LOC’ (location approved for drilling) are omitted.
4. The first month in which the well shows nonzero oil or gas production is in January 2005 or later. A ‘FirstProdDate’ field was added to the production table and was filled with the earliest report date in which either the ‘BBLS_OIL_COND’ OR ‘MCF_GAS’ field was greater than zero. A ‘MonthProd’ field was then calculated to be the age of the well.

5. The well is listed as 'horizontal' in the wellbore field of the wellindex table. Wellbores listed as 'vertical' or 'horizontal re-entry' are omitted. While a horizontal re-entry well may represent re-completion of an existing well into the Bakken formation, these wells are very few in number and were considered non-representative.

Henceforth, the wells meeting the above criteria (7271 wells in total) will be called "Bakken wells." We believe that this number represents the vast majority of the wells reasonably considered to be Bakken wells drilled in the study time period. Because no definitive list of "Bakken wells" is published, we cannot be certain about the level of omissions.

2.2.3 Cleaning and Organization of Well Property Data

A number of steps were required to clean and organize well property data before input into the OPGEE model. In cases where a central estimate is required, we use the following logic:

- The production-weighted mean (or production-weighted average) is used where an intensive quantity of interest (e.g., volume of gas flared per bbl of oil produced) should not be averaged because of large differences in the denominator (normalizing quantity).
- The mean was used in cases where the data did not appear to be highly skewed, while the median was assumed to be a better measure of typical behavior if the distribution was skewed.

2.2.3.1 Well Geometry and Casing Characteristics

The wellmaster file contains multiple records for a given well, each for a different well segment or "pipe type." Each record contains a "top," "bottom," and "diameter" for each well segment. Each record also enumerates the DTD (drilling total depth) and, in some cases, the TVD (true vertical depth) for the well as a whole. The wellmaster file was modified in MySQL to combine fields for each well. Well segments were organized into fields by the casing or segment name: 'SURF' (surface casing); 'PROD' (production casing); 'COND' (conduction casing); 'L1', 'L2', and 'L3' (laterals 1, 2, and 3); and 'CSG' (miscellaneous casing).

A small number of wells lacked an entry for DTD. If no information was given, median DTD was used. In other cases, the DTD was calculated by taking the maximum value for the "bottom" across all casing types.

In a small number of cases, data entries for top and bottom of casings appeared to have been reversed or entered in error, resulting in negative computed casing length. All entries were corrected using other available information. If a surface casing depth was not reported, the well was adjusted to have a surface casing with a casing bottom of 2076 feet and a diameter of 9.625 inches (mean values for reported surface casings).

The American Petroleum Institute (API) has defined standard casing diameters [12]. In casing sections where the reported diameter deviated from an API standard, the casing was adjusted to the closest standard diameter. Some wells were found to have a casing diameter of zero for some segments of casing. These instances were corrected to the most common casing diameter for that segment, using API casing diameters and information from the great majority of wells that reported casing diameters [12].

OPGEE requires an input of the TVD of each well to compute the work of fluid lifting. Few wells (<100 wells) in DMR datasets reported TVD. Therefore, to complement the DMR dataset, the FracFocus database was mined for both TVD and fracturing water consumption information [13]. Data were obtained using an automated script for all wells in our database that were also available in FracFocus datasets.

In cases where both FracFocus data and DMR data existed for TVD, the FracFocus value was chosen. FracFocus data were chosen as the default because of poor reporting of TVD in DMR datasets. The remaining unreported TVD values were estimated via analytical methods. For wells with reported TVDs, a robust trend was found between TVD, the coordinate of the top of the lateral casing, and the coordinate of the bottom of the production casing. Assuming that the top of the lateral casing was at the beginning of the curved well section, the radius of curvature can be estimated by the following equation (see Figure 1):

$$r = TVD - L_{1,Top} \qquad \text{[ft]}, \tag{1}$$

where TVD is the true vertical depth and $L_{1,top}$ is the depth of the top of the first lateral casing section (generally the only lateral casing section). Similarly, assuming that the production casing extends through the curve to the beginning of the horizontal section, the radius of curvature can be estimated as follows:

$$r = \frac{(Prod_{Bot} - TVD)}{\left(\frac{\pi}{2} - 1\right)} \qquad \text{[ft]}, \tag{2}$$

where $Prod_{Bot}$ is the bottom of the production casing. Averaging across all wells with complete information, using both methods, the mean radius of curvature was found to be 616 ft.

Unreported TVD values were therefore calculated, assuming a mean radius of curvature of 616 feet, via both the methods above (production bottom and lateral top); the deeper of the two values was the value used for TVD. Lastly, for the small subset of wells (36 wells) that did not provide enough casing information to calculate TVD, the mean reported TVD value of 10,354 feet was used.

For consistency, casing lengths were adjusted such that the production casing ended no earlier than the beginning of the horizontal section and the lateral casings began no later than the beginning of the turned section.

We show input distributions for computed TVD and DTD in Figure 2 and Figure 3, respectively. DTD as a function of time is plotted in Figure 4 for all wells in our dataset. Because most wells have a TVD of about 10,000 ft, the plot of DTD in Figure 4 can be used to understand the change in lateral length over time. Subtracting 10,000 ft vertical depth from reported DTDs, Figure 4 shows a shift from a variety of lateral lengths (before January 2007) to an even mix of 5,000-ft and 10,000-ft laterals (Jan. 2007–Jan. 2010), to a situation dominated by 10,000-ft laterals (after Jan. 2010).

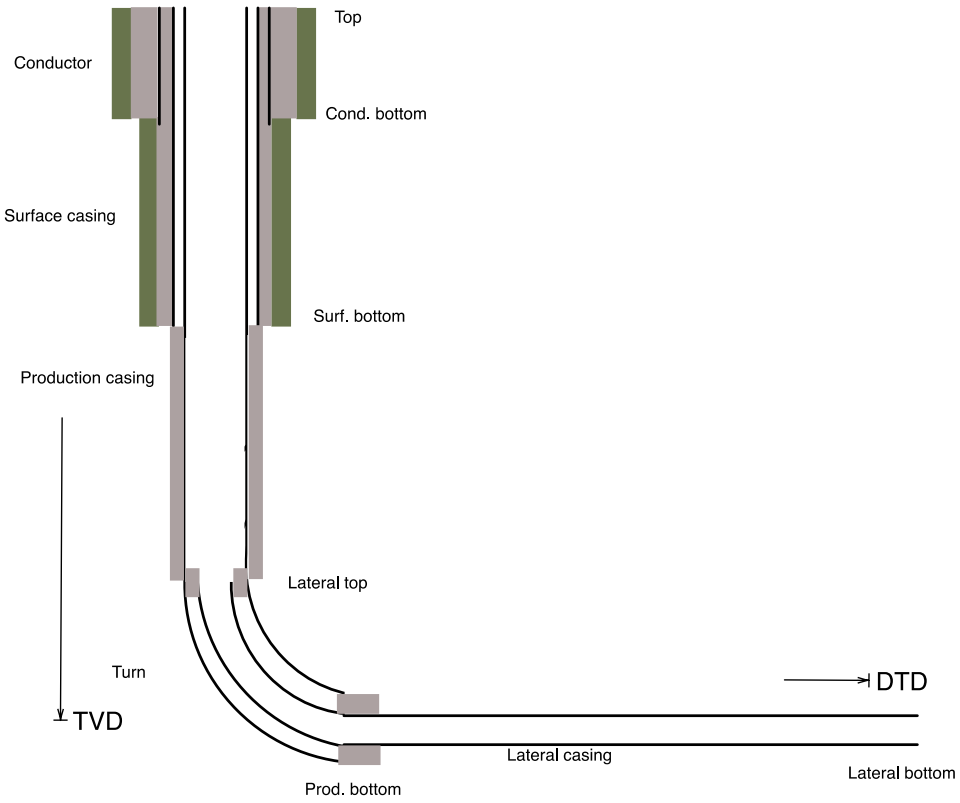

Figure 1. Bakken well diagram with key depth markers listed.

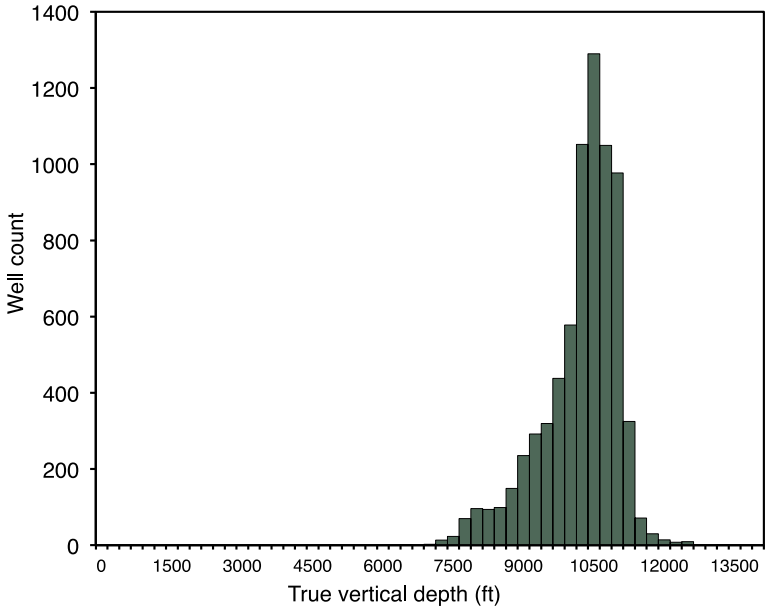

Figure 2. Distribution of true vertical depths (ft) for Bakken wells.

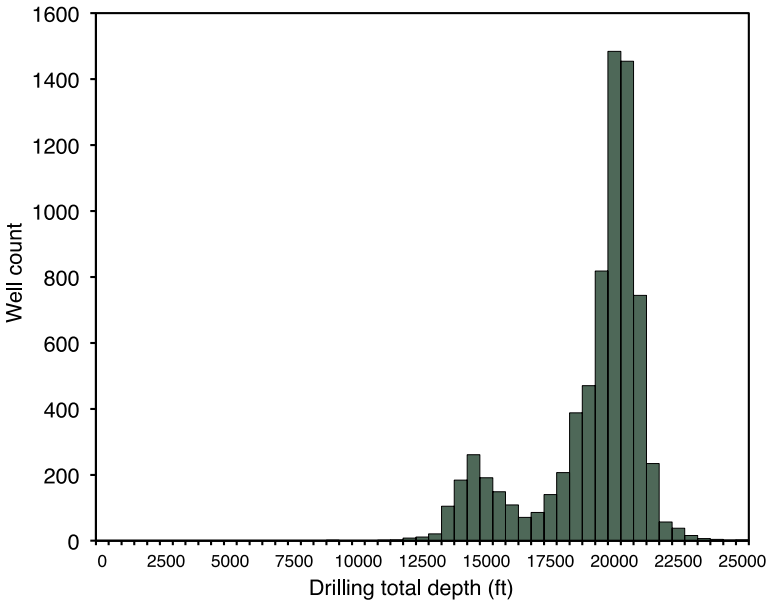

Figure 3. Distribution of drilling total depths (ft) for Bakken wells.

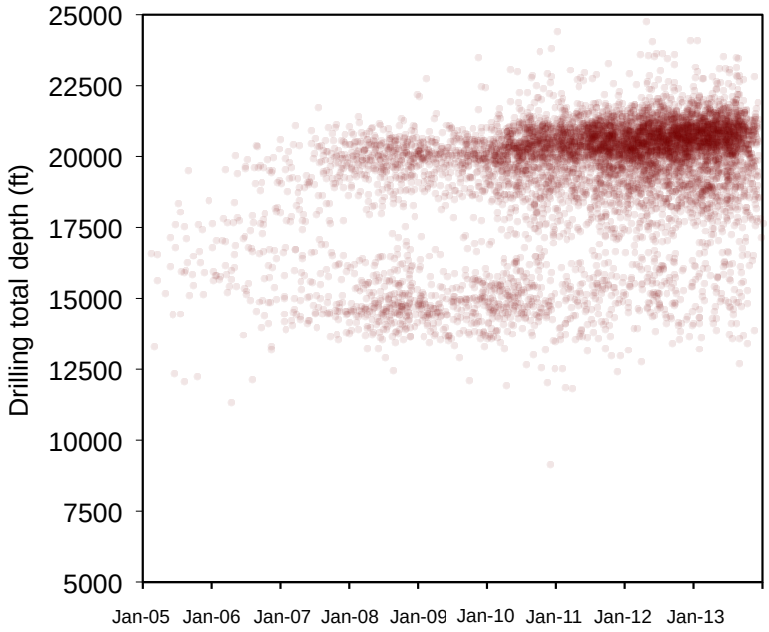

Figure 4. Drilling total depth for wells in database as a function of time. Most wells have TVD of 10,000 ft, so DTD less 10,000 ft is the approximate lateral length. Before Jan. 2007, a mix of lateral lengths prevailed. Between Jan. 2007 and Jan. 2010, roughly equal numbers of wells with 5,000-ft laterals (DTD ~ 15,000) and 10,000-ft laterals (DTD ~ 20,000) existed. After 2010, most new wells had a lateral length of 10,000 ft (DTD ~ 20,000).

2.2.3.2 Fracturing Water and Sand Use

One value of interest is the volume of water used in fracturing wells. We used two primary sources for fracturing water volume, the DMR geostimulations dataset and the FracFocus dataset [13]. Both of these datasets report one-time fracturing water usage (as compared to monthly produced water volumes reported in DMR production datasets). As the reported DMR and FracFocus water volumes for the same well often diverged, the larger of the two values was used to be conservative. However, if one volume value was reported as over 20 million gallons, the smaller of the two values was used instead of the larger. The value of 20 million gallons was chosen for this threshold because it was the maximum value that was reported consistently for the same well across both datasets. Where neither dataset reported water consumption, the mean reported value of 2.614 million gallons was used. A total of 2840 wells were set equal to this mean value. The rate of recycling of fracturing water is unknown. The distribution of water use in Bakken wells (except those set to default) is plotted in Figure 5.

The sand used as fracture proppant was reported in the DMR geostimulation table in units of pounds. To examine outliers or misreported data, the pounds of sand injected was plotted against the gallons of water used in fracturing on a log-log scale. Outliers were assigned estimated sand amounts using the average sand/water ratio of 1.0687 [lb proppant/gal of water]. If neither sand nor water data were reported, the average sand/water ratio was applied to the average water consumption above (284 wells were set equal to this value). The distribution of proppant use in Bakken wells (except those set to default) is plotted in Figure 6.

The fracturing pressure gradient was calculated by taking the value of fracturing pressure from the geostimulations dataset (in psi) divided by the TVD as computed above. The average gradient was found to be 0.78 psi/ft. This figure aligns well with data reported in other sources, which range from 0.76 to 0.85 psi/ft [14, 15].

Table 4 gives a summary of the above well property data and characteristics of the property distributions.

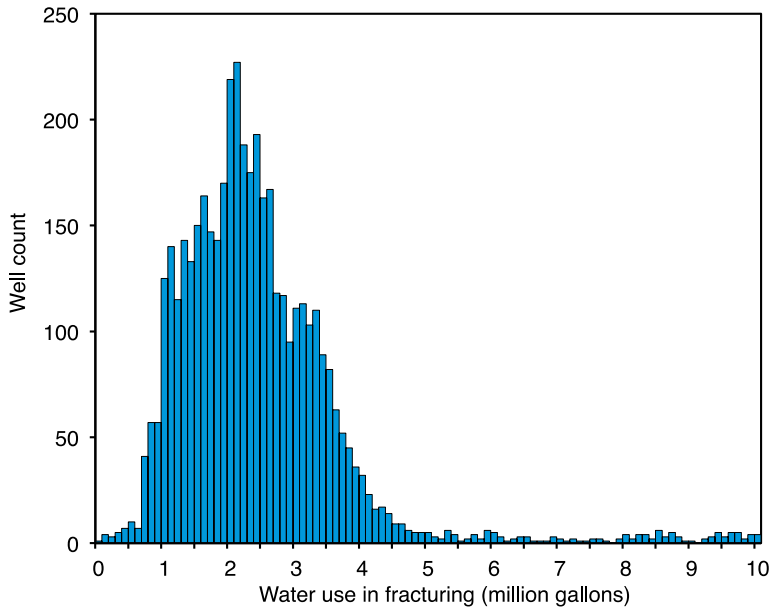

Figure 5. Distribution of water use in hydraulic fracturing (million gallons, one-time use). See above for methods of computation of average value and removal of outliers. Some values are to the right of the edge of the plot.

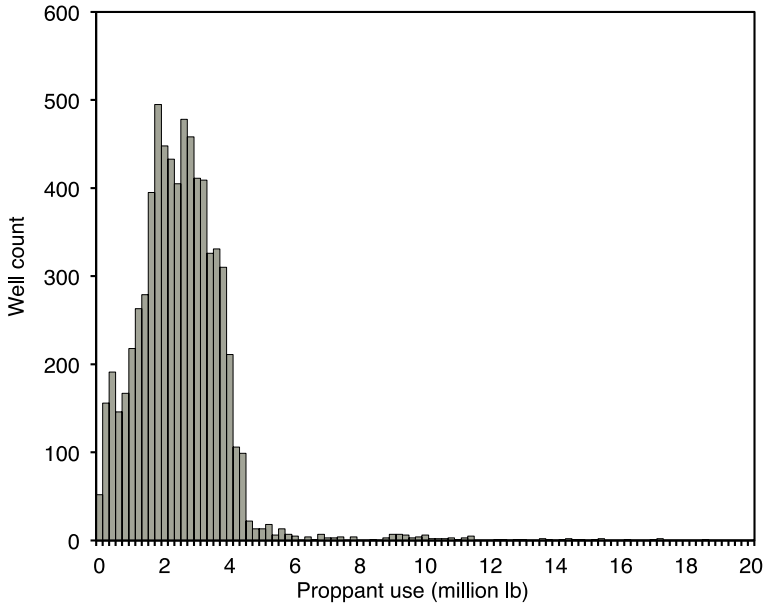

Figure 6. Distribution of proppant use in hydraulic fracturing (million lb of proppant, one-time use). See above for method of computation of average value.

Table 4. Well property input data summary

Property	Median	Mean	Std. Dev.	Units
API Gravity	41.90	41.93	2.05	[deg. API]
True vertical depth (TVD)	10,533	10,352	806	[ft]
Drilling total depth (DTD)	20,154	19,397	2,141	[ft]
Fracturing gradient	0.79	0.79	0.23	[psi/ft]
Fracturing pressure	8,315	8,149	2,519	[psi]
Fracturing sand consumption (one-time)	2,533,560	2,598,586	1,559,650	[lb]
Fracturing water consumption (one-time)	2,280,096	2,615,134	1,816,970	[gal]

2.2.3.3 Gas Composition

Because gas composition is reported for only a fraction (< 10%) of wells in the dataset, and because the tests for gas composition that were reported were performed at different times throughout a well's depletion profile, it is not possible to determine a reliable gas composition for each well. Therefore, we use the mean gas composition of all of the reported gas tests for the gas composition of all wells in the Bakken. This composition is shown in Table 5. At this composition, the lower heating value (LHV) of the gas is 1500.3 Btu LHV/scf [16]. Less than 33% of the heating value of Bakken-produced gas is provided by methane (910 Btu/scf CH_4 multiplied by 0.492 scf CH_4/scf raw Bakken gas).

Table 5. Mean gas composition (raw gas before processing) in reporting wells

	CO_2	N_2	C_1	C_2	C_3	I-C_4	N-C_4	I-C_5	N-C_5	C_6	H_2S	O_2, Ar
Mol %	0.70	3.67	49.24	21.03	15.09	1.68	5.06	0.90	1.26	1.65	0.005	0.02

2.2.3.4 API Gravity

API gravity can be reported multiple times over the life of a well. For each well, all API gravity test results reported were averaged together. First we converted API gravities to specific gravity, averaged the results, then calculated the API gravity associated with this mean specific gravity. Similarly, the mean specific gravity was calculated for all samples in all wells. The resulting mean API gravity of 41.90 was used for all wells with no API gravity reported (a total of 1922 wells). The distribution of API gravity results, except those set to default value, are shown in Figure 7.

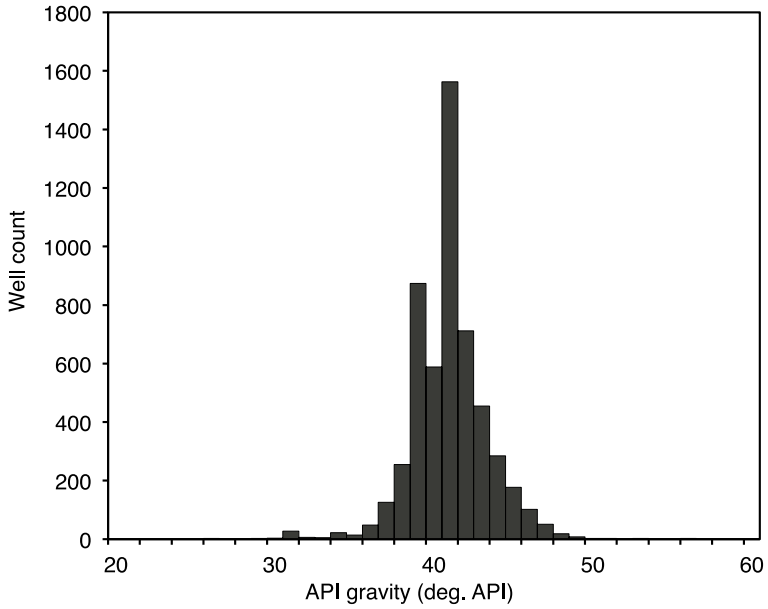

Figure 7. Distribution of API gravity of Bakken crude oil for reporting wells (wells set equal to mean API gravity are removed from distribution). See above for method of computation of average API gravity.

2.2.4 Estimation of Lifetime Well Productivity

Well productivity data are estimated using production decline models that are well established for use in the Bakken formation. McNally et al. fit a total of 5773 wells in the Bakken formation to two- and three-parameter versions of the Hyperbolic Decline (HD) and Stretched Exponential (SE) depletion models [17, 18]. Least-squares fitting methods were applied to each well for each model type. The results of each model fit were compared using

statistical model comparison tools (corrected AIC score). See prior work for details of this fitting process [17, 18]. An example fit is shown in Figure 8.

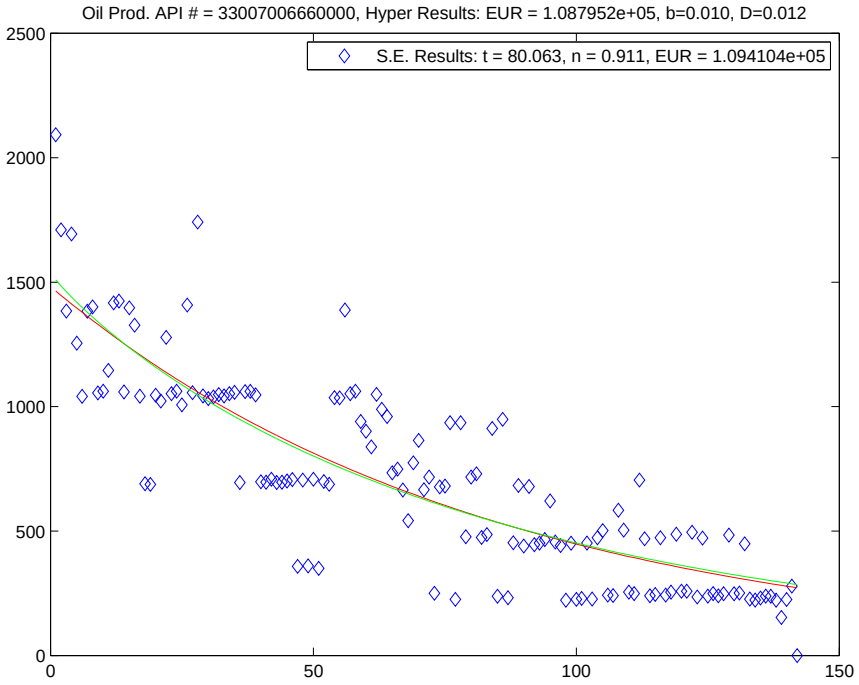

Figure 8. Example fit of oil production (y-axis, bbl per day) as a function of month of production (x-axis).

In this work, two-parameter HD and SE decline curve models are applied to estimate oil, gas, and water production over the life of each well. For each model and well, three projections are made, for 15-, 30-, and 60-year well lifetimes, respectively. In this study, the 30-year well lifetime is used as the default result. Because of the rapid decline of all fluid production from these wells, the difference between 15-, 30- and 60-year values is not as large as might be expected [17, 18]. McNally and Brandt [17] found that the HD and SE models worked approximately equally well using standard statistical methods of fit comparison (corrected AIC). For this reason, in this study each estimated ultimate recovery (EUR) is the average of the 30-year HD and 30-year SE model fits. The number of wells in the dataset in this study is larger than the number in the dataset of McNally and Brandt [17], and not every well in that dataset is represented in this dataset. Therefore, to all wells in this study with no fitted EUR (a total of 1995 wells), we assign the median result from all fitted wells, as shown in Table 6. The median was used in preference to the mean because of the large right-tail in the EUR distribution, which pulls the mean well above the "typical" or median well.

Figure 9 shows the distribution of fitted crude and condensate EUR values in units of 1000 bbl. The distribution of fitted estimated lifetime GOR for each well is shown in Figure 10. The distribution of fitted estimated lifetime water-oil-ratio [bbl water/bbl oil] is plotted in Figure 11.

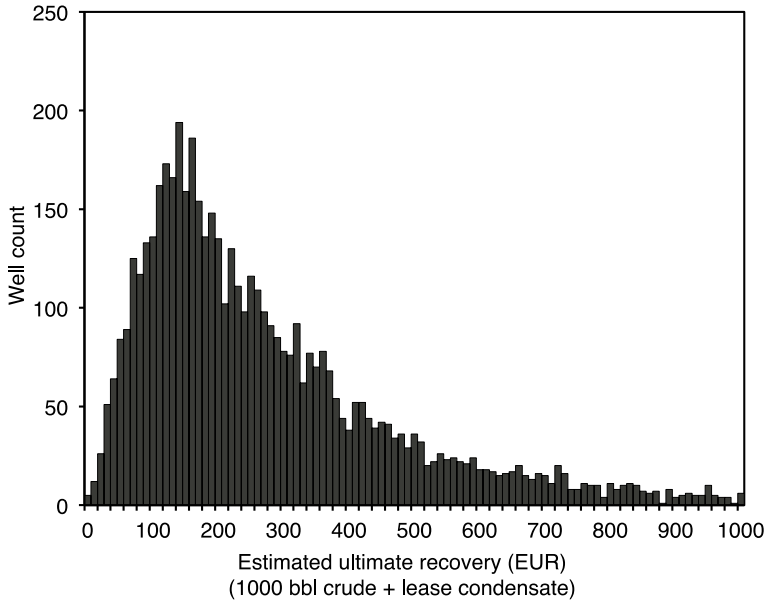

Figure 9. Distribution of estimated ultimate recovery of crude oil + condensate (1000 bbl). A total of 114 wells are off the right side of the plot, with greater than 1 million bbl EUR. See above for method of computation of EUR.

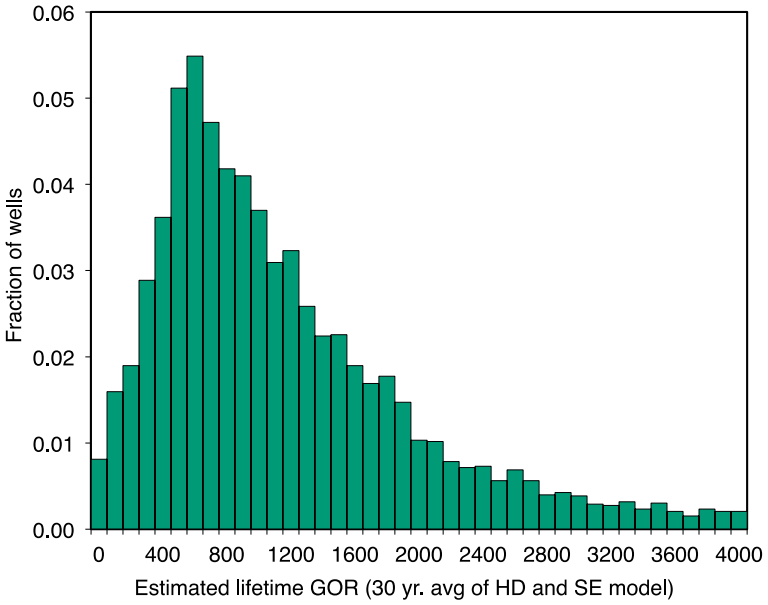

Figure 10. Distribution of estimated lifetime GOR. Result is based on average of 30-year HD and SE decline curve models for oil and gas.

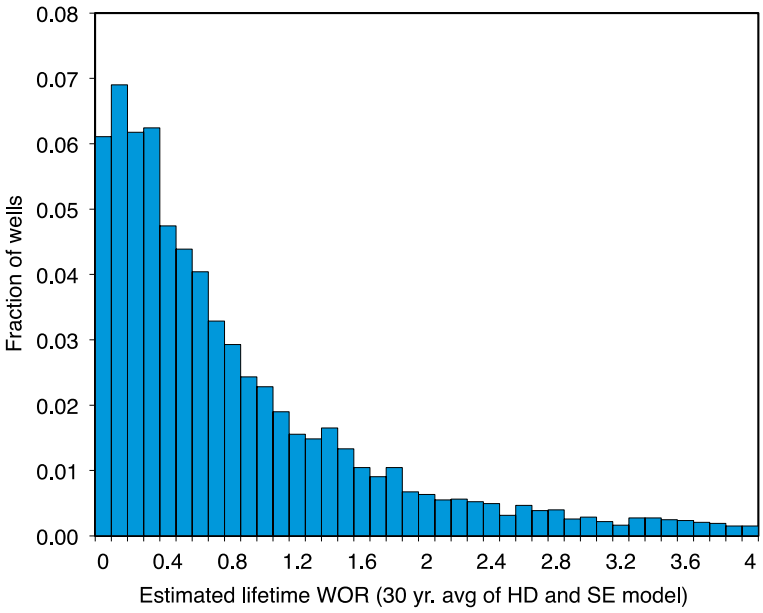

Figure 11. Distribution of estimated lifetime WOR using HD and SE fitting models. Result is based on average of 30-year HD and SE decline curve models for water and oil.

Table 6. Estimated ultimate recoveries of oil, gas and water, along with estimated lifetime GOR and WOR values. Each fitted model is the average of 30-year lifetime estimated production profiles, based on an average of HD and SE models fit to each time series.

	Oil EUR (bbl)	Gas EUR (mcf)	Water EUR (bbl)	GOR (scf/bbl)	WOR (bbl/bbl)
Mean	279,080	355,165	215,935	1,524	1.13
Prod-weighted mean	279,080	355,165	215,935	1,273	0.77
Median	226,088	252,973	139,305	1,119	0.62
5%-ile	72,768	52,877	24,730	330	0.08
25%-ile	166,481	168,295	92,252	777	0.39
75%-ile	308,347	364,499	205,873	1,423	1.01
95%-ile	697,062	1,009,919	702,208	3,861	3.76
Mode	226,088	252,973	139,305	1,119	0.62

2.2.5 Drilling Model Inputs

A number of data inputs are required for use of the improved drilling and fracturing module (described below). In order to estimate the drilling energy use from fundamental physical relationships, the following data are required:

- The type of drilling equipment used;

- The typical rates of penetration;
- The typical rates of torque applied to the drill string by the top-drive system;
- The typical rates of pressure drop through the downhole mud motor; and
- The typical rates of drilling-mud circulation.

Each of these parameters can vary for the vertical and horizontal sections.

A number of sources suggest that the drilling equipment used in the Bakken has changed significantly since the onset of modern development in 2005. Current best practice involves the use of a top-drive system for applying torque to the drill string [19]. This top-drive system is typically used to generate drill string rotation speeds of ~60 RPM (range 55–75 RPM) [20, 21]. In addition to rotation of the drill string, rotational energy at the bit is supplied by the circulation of drilling fluid (mud), which forces the drilling mud through a downhole motor, causing additional rotation of the drill bit beyond that supplied by the drill string. Use of downhole motors enables the steering required to shift from vertical to lateral drilling and to steer the (often long) lateral of the well to maintain contact with the Bakken formation. Mud motor rotation speeds are typically ~180 RPM (range 160–200 RPM) [20, 21]. Therefore, total bit rotation speeds are ~240 RPM (range 200–275 RPM). Top-drives and mud pumps are driven by electrical connections to large diesel- or gas-fired generator sets (e.g., Caterpillar oilfield generator sets).

The rate of penetration (ROP) varies greatly along the length of the well. Near-surface penetration rates can exceed 500 ft/hr [20], dropping to 40–80 ft/hr in the bottom part of the vertical section [20, 22]. Penetration speed depends on rock type, bit wear, rig power, and numerous other factors. Drillers aim to increase penetration rates, and have successfully done so as they have become more experienced in the Bakken play. ROP in the lateral section tends to be lower than vertical ROP, with highest ROPs reported at ~120 ft/hr, and more typical ROPs reported from 35 to 80 ft/hr, [22] [23] [24; Figures 7, 8, 9] [25]. Therefore, the following ranges are specified for ROP in the Bakken:

- Vertical: base case = 110 ft/hr (range = 50–220 ft/hr)
- Horizontal: base case = 80 ft/hr (range = 40–120 ft/hr)

Torque applied to the drill string supplies some of the energy for cutting. The torque applied can vary greatly over different portions of the well drilling process (e.g., owing to sticking of string or stalling of drilling). A range of torques for Bakken drilling were noted in the literature [21, 24, 26, 27]. Using these data, the following base case and ranges for top-drive surface torque were applied:

- Vertical: base case = 9000 ft-lb (range = 8000–10000 ft-lb)
- Horizontal: base case = 12000 ft-lb (range = 9000–13000 ft-lb)

Pressure drop through the mud motor provides the rotational energy to the bit (in excess of that applied by drill string rotation). The energy consumed by the mud motor can be calculated using the mud pressure drop and the mud circulation volume. Mud pressure drops are reported in a variety of cases for Bakken wells [20, 24]. Horizontal-drilling mud pressure drops reported are higher than vertical-drilling mud pressure drops. Using these data, the following base cases and ranges for mud pressure drop through the mud motor were applied:

- Vertical: base case = 500 psi (range = 450–550 psi)
- Horizontal: base case = 700 psi (range = 400–1200 psi)

Rates of mud circulation, typically reported in gallons per minute (gpm), were derived from multiple sources [20, 24]. Higher rates of mud circulation are required in laterals to successfully remove rock fragments. Rates of mud circulation are as follows:

- Vertical: base case = 200 gpm (range = 150–400 gpm)
- Horizontal: base case = 500 gpm (range = 420–550 gpm)

2.2.6 Flowback of Hydraulic Fracturing Fluids

Hydraulic fracturing requires injection of fracturing fluids, which are primarily water and sand, with small amounts of other chemicals added (biocides, corrosion inhibitors, lubricants, viscosity-adjusting agents). After hydraulic fracturing occurs, fracturing fluids are returned to the surface in order to allow production of reservoir fluids to begin. The injected fluids are returned to the surface, along with some gaseous and liquid hydrocarbons from the formation (increasing during the flowback period). Flowback takes a variable amount of time, from hours to weeks, depending on the well and its characteristics. Flowback of produced gas can cause climate impacts (GHG emissions) if not handled correctly [28, 29, 30].

Flowback is performed with low-pressure separation equipment in place, owing to the need to avoid backpressure on the wellhead, which would retard the movement of the flowback fluids to the surface. Options for managing flowback fluids (gases in particular) include the following:

- Depositing fluids into atmospheric-pressure holding tanks and venting of associated gas in the tank headspace;
- Flaring of associated gas that is produced with flowback fluid; and
- Use of a three-phase low-pressure separator that is able to handle produced materials (e.g., produced sand) to send produced flowback gas to the sales line.

Industry reporting to the EPA Greenhouse Gas Reporting Program (GHGRP), as analyzed by the Environmental Defense Fund (EDF) [31], suggests that flowback gases are flared in the Bakken formation. A total of 88 completion events in McKenzie and Williams

counties were reported to the federal GHGRP program as horizontal wells (almost certainly Bakken wells). All wells reported flaring of flowback methane. No wells reported use of separators for sales of flowback gas. This suggests that flaring of flowback gas is the most common management scheme in the Bakken formation.

Flowback volumes have been modeled in a variety of sources [31]. The most common approach, used by O'Sullivan [28, 30] and the EDF, is to scale flowback emissions using initial production. For example, O'Sullivan assumes that flowback occurs for 9 days on average, and that production of gas increases linearly, resulting in 4.5 days of equivalent initial production as flowback gas. EDF, in contrast, assumes non-linear increases of gas over 7–10 days. This model results in an equivalent of 3 days' worth of initial gas production emitted during flowback [31].

We adopt a similar approach here, using 3 and 4.5 days to bracket the low and high estimates of flowback volumes. Two approaches could be used to estimate daily production. One approach would be to take the first month's reported gas production and divide this amount by the number of days of production in the first month. However, operators in the Bakken also report initial production test (IPT) results for oil, water, and gas volumes produced. A total of 5505 wells were found in IPT databases that were also included in our subset of modeled Bakken wells. The largest estimated flowback volume in the dataset was removed as an outlier before computing summary statistics. This outlier well reported flowback 50 times larger than the next largest volume reported, and amounting to over $27 million worth of gas (3–4 times the drilling cost of a typical Bakken well). We therefore consider this result to be a data entry error.

In our base-case analysis, we assume that 3 IPT days' worth of production is produced during flowback. The resulting distribution of flowback volumes is shown in Figure 12. Distribution characteristics are reported in Table 7. The implied daily volumes based on IPT test results tend to be higher than those based on first-month produced volumes prorated by operating days (mean multiple = 4.5).

For analysis in OPGEE, we generate flowback volumes per barrel produced by dividing our estimate of flowback gas based on IPT data by the volume of oil EUR (per well, modeled as described above). When pro-rated over all barrels of oil produced over the life of the well, Bakken flowback flaring volumes tend to be small compared to operational flaring in the Bakken formation. Distribution characteristics for per-bbl flowback volumes are reported in Table 8.

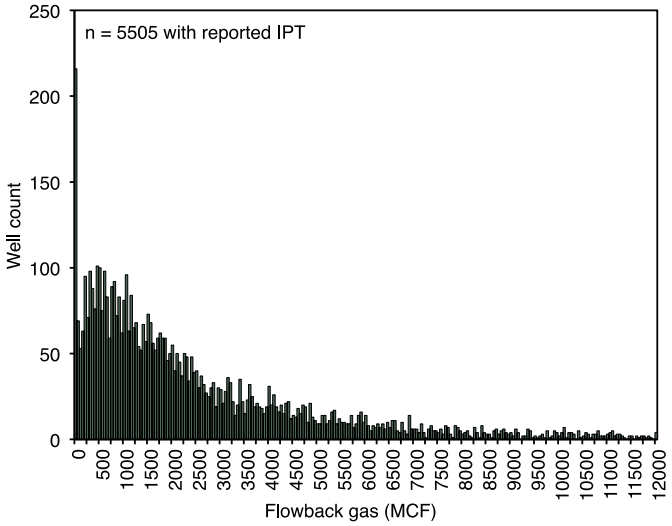

Figure 12. Distribution of flowback gas volumes based on initial production test data for 5505 reporting Bakken wells.

Table 7. Flowback volume distribution information for reporting IPT wells (n=5505, less one outlier)

	Flowback Volume (mcf)	
	3-day-equivalent	4-day-equivalent
Mean	3007	4510
Median	1763	2644
Std. Dev.	4362	6543
Min	0	0
Max	133704	200556
5%-ile	93	140
25%-ile	759	1139
75%-ile	3727	5590
95%-ile	10195	15292

Table 8. Flowback volume per bbl produced (EUR) for reporting IPT wells (n=5505, less one outlier)

	Flowback Volume per bbl (scf/bbl)	
	3-day-equivalent	4-day-equivalent
Mean	15	22
Median	7	11
Std. Dev.	22	33
Min	0	0
Max	752	1128
5%-ile	1	1
25%-ile	3	5
75%-ile	16	24
95%-ile	47	71

2.2.7 Other Emissions Data

Few data are available on direct emissions from Bakken operations that are not associated with energy use or process operations that can be modeled. There is some evidence that sources of methane emissions might be important in the Bakken region. For example, airplane-based sampling in the Bakken has shown the existence of methane plumes separate from plumes associated with flare combustion products [9, 32]. The source of these methane plumes is unknown.

Possible sources of direct emissions include the following:

- Standing and working losses from crude oil and hydrocarbon storage tanks;
- Standing and working losses from produced-water tanks;
- Leaks and fugitive emissions at the wellhead;
- Leaks and fugitive emissions from process equipment, gathering systems, etc.;
- Leaks and fugitive emissions from field compressors; and
- Incomplete combustion in flares.

Because no experimental data are available on these emissions sources that are specific to the Bakken region, the OPGEE default values are used unless otherwise noted. For OPGEE v1.1 draft D, as set to OPGEE default values in all other characteristics, the venting and fugitive emissions leakage rate amounts to 35.1 scf/bbl. This loss rate equals about 3.1% of the median Bakken GOR of 1119 scf/bbl. Owing to lack of more specific data, this venting and fugitive emissions rate is applied to all Bakken wells.

2.3 Analysis Methods

This section describes the methods by which collected data were input into the OPGEE model and drilling model. OPGEE v. 1.1 draft D is used [33]. Each section below describes model modifications and any remaining data sources.

2.3.1 Drilling

OPGEE v. 1.1 draft D contains only a simple relationship for energy to drill a well as a function of well depth [33]. It does not include any treatment of horizontal wells. In order to address these shortcomings, OPGEE is augmented in the following ways:

1. The function to compute energy use in drilling a well is replaced with a well-specific energy consumption value computed using an auxiliary model, GHGFrac (see below).
2. The OPGEE default lifetime productivity in bbl of oil per well is replaced with a well-specific EUR computed using above-described decline curve methods.

3. These results are used to compute the fractional energy consumption in drilling, in Btu consumed for drilling per Btu of oil EUR.

To estimate the energy used in drilling and hydraulically fracturing wells in the Bakken, we use the GHGFrac model. GHGFrac is an open source model for estimating the GHG emissions from hydraulic fracturing. This model was developed by Vafi and Brandt at Stanford University [34]. GHGFrac addresses the significant sources of on-site emissions, including drilling of wells and injection of fracturing fluid. The model covers drilling of vertical and directional wells, mud circulation, cementing, and draw work, as well as injection of water for fracturing. The model can handle arbitrary well geometries for wells that consist of many sections with different inclination angles.

The energy used for drilling is consumed partly to rotate the drill string and partly to circulate mud during drilling. The user has the option to select top-drive rotation, downhole motor, or a combination as the source of rotational motion of the drill bit. The rotational drilling model has three modes: empirical, user-defined torque, and automatic torque factor computation. The empirical model uses a torque factor as suggested by Azar and Samuel [35]. In the user-defined torque mode, the user can define the torque value for each section of the well to drill, which is useful for situations where applied torque is available from collected data. The automatic torque computation mode uses a "soft string" model based on Mitchell and Miska's method to calculate the required torque for directional drilling [12]. GHGFrac models mud circulation, as the mud pump is a significant source of energy consumption. Mud is a non-Newtonian fluid; GHGFrac considers the rheology of mud to calculate the pressure drop of mud flow due to pipe friction. GHGFrac includes the "Bingham plastic" and "power law" models to describe the rheology of mud. The model automatically computes the critical velocity required for effective removal of the drill bit cuttings and then can calculate the required flow rate of mud.

The hydraulic fracturing model uses the fracture gradient of the formation as an input variable. The fracture gradient is measured in [psi/ft] and represents the pressure required to fracture rock as a function of well depth. Using the fracture gradient and a hydraulic model, GHGFrac calculates the required discharge pressure of the water injection pumps. Given the volume of the injected water, the total energy required to apply the required pressure is calculated. This model considers variable diameters of different sections of the well as the water flows from the surface to the horizontal section of the well, and includes fluid flow into the reservoir. The hydrostatic pressure of water in a deep wellbore reduces the required discharge pressure of the pump, which is included in GHGFrac.

Cementing is a dynamic operation in which the levels of cement and mud change with time. Owing to the differing densities and other properties of mud and cement, cementing is a more complicated phenomenon to model than mud circulation. The cementing model approximates cementing energy by splitting the dynamic cementing problem into six steady-state snapshots to reflect the positions of the mud and cement levels in the well. The well geometry can consider the different sections with different inclination angles. The result of the model is compared with field data and the classic model of Slagle [36]. Energy consumption during cementing is small because of the short time for injection of cement compared with the drilling

operation. The order of magnitude of energy required for tripping out the drill string has also been found insignificant compared with that for hydraulic fracturing, drilling, and mud circulation.

For the detailed mathematical description and verification of the model, please see Vafi and Brandt [34].

2.3.2 Production Methods

Bakken crude oil is first produced via pressure depletion (primary production) and flowback of fracturing fluid. Owing to rapid pressure decline (see below), Bakken wells use artificial lift to increase production. Typical implementations use downhole pumps (sucker-rods). We assume for simplicity that all producing wells use artificial lift, although many wells will require little to no energy for lift in the early portions of production given the high initial bottom-hole flowing pressure P_{wf}. All artificial lift is assumed to be supplied by downhole pumps rather than gas lift.

While some experimentation is currently being performed on CO_2 injection for enhanced recovery in the Bakken formation [37, 38], we assume that no fluids are reinjected into the surface (e.g., no gas or water reinjection; no gas, water or steam flooding). DMR datasets support this assumption, with a lack of reported injection information for Bakken wells [1].

Table 9 shows the default OPGEE inputs for production methods as well as the assumed OPGEE inputs for the Bakken case.

Table 9. Production method inputs

Data Input	OPGEE Default	Bakken Value	Freq. of Variation	Source	Notes
Downhole pump	1	1	No change		Downhole sucker-rod pump
Water reinjection	1	0	"	[1]	No water injection reported in DMR dataset
Gas reinjection	1	0	"	[1]	No gas injection in DMR dataset
Water flooding	0	0	"	[1]	No water injection in DMR dataset
Gas flooding	0	0	"	[1]	No gas injection in DMR dataset
Gas lifting	0	0	"		No gas lift technology assumed
Steam flooding	0	0	"	[1]	No steam injection in DMR dataset

2.3.3 Reservoir Properties

The field location is "US Continental," and the field name is "Bakken." The depth of the well is the TVD (as computed above). The production volume is the oil production volume for each month (as computed above). The well diameter is the reported production tubing diameter.

North Dakota Bakken initial reservoir pore pressure gradients range from 0.58 to 0.8 psi/ft [15]. The initial pressure gradient in all Bakken wells is assumed to be 0.7 psi/ft, where the depth of the well is defined by the well TVD. Pressure declines over time, resulting in the need for additional energy input in the form of artificial lift.

The productivity index (PI) of Bakken wells is not widely reported. The PI is the amount of oil produced per unit time per unit of pressure drawdown between far-field reservoir pressure and the flowing bottom-hole pressure. It is a measure of the resistance of the formation to flow. The PI is difficult to characterize for a formation like the Bakken, and will vary significantly with the effectiveness of the fracturing process. Reported values range from effectively 0 to 0.2 bbl/day-psi [39]. Because of uncertainty about the PI, an approach based on a simple model of bottom-hole flowing pressure, rather than a model relying on reservoir pressure and productivity index, is used.

Pressures over time are not reported in DMR datasets. Pressure decline curves are only published for a limited number of examples of Bakken wells [37, 40, 41, 42]. Tabatabaei et al. [40, Figure 3] show a decline from initial P_{wf} to a plateau at 3000 psi. Tran [41, Figure 4.2] shows a decline to 1000 psi followed by a plateau. Kurtoglu [37, Figure 8.7] shows pressure starting at 6000–8000 psi and declining to 2000 psi over 450 days. Yu et al. [42, Figure 4] develop a synthetic log-linear model of P_{wf} as a function of time. This model was developed as a synthetic pressure trend for reservoir simulation, but is thought to be reasonably representative of behavior in the Bakken. On the basis of this model, we assume that the initial bottom-hole flowing pressure $P_{wf,i}$ is 500 psi less than the initial reservoir pressure. Pressure then declines over time as a linear function of the log-transformed day of production until a minimum P_{wf} of 1000 psi is reached and maintained for the life of the well. Fitting the plotted results of Yu et al. [42], we find that

$$P_{wf}(d) = max\{P_{wf,i} - 2350 \times \log_{10}(d) \mid 1000\} \quad \text{[psi]} \tag{3}$$

Depending on the initial reservoir pressure, this results in a decline in the initial reservoir pressure to 1000 psi over approximately 1 year. Of course, any given well will differ from this simple model, but this is believed to be a reasonable approximation for a typical Bakken well. Figure 13 shows the results for this equation for an example well using linear and logarithmic time axes. Table 10 Table shows the default OPGEE inputs for field properties as well as the assumed OPGEE inputs for the Bakken case.

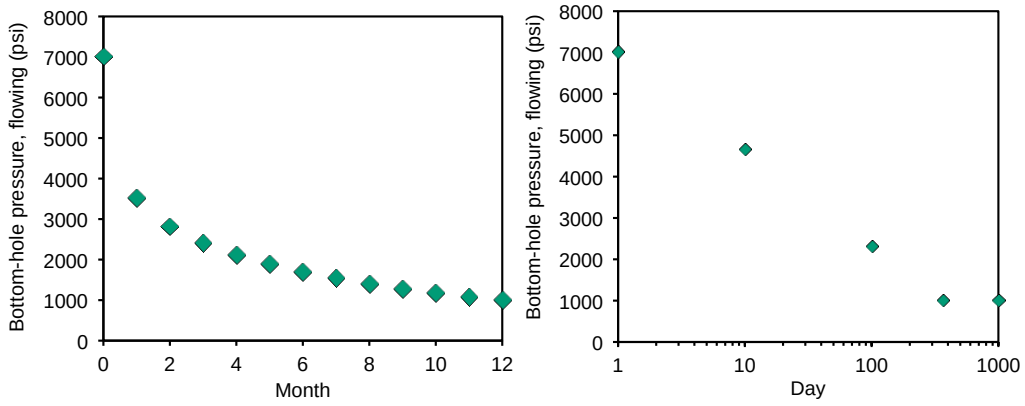

Figure 13. Pressure (bottom-hole flowing, P_{wf}) as a function of time for example well starting at P_{wf} = 7000 psi. Left: Time in months, linear scale. Right: Time in days, log scale.

Table 10. Field properties inputs

Data Input	OPGEE Default	Bakken Value	Freq. of Variation	Units	Source	Notes
Field location (country)	Generic	US Continental	No change	-	-	
Field name	Generic	Bakken	"	-	-	
Field age	35	Well age	"	[y]	[2]	Well age in months divided by 12
Field depth	7240	Well TVD	"	[ft]	[2]	Well TVD computed using method noted above
Oil production volume	1500	Well prod.	"	[bbl/d]	[1]	Well oil production computed using method noted above
Number of producing wells	8	1	"	-	[2]	Per well
Number of water-injecting wells	5	0	"	-	[2]	No water injection
Well diameter	2.75	2.75	"	[in]	[2]	All production tubing same diameter
Productivity index	3	-	"	[bbl-d/psi]	-	Not used. Instead, use above method to compute P_{wf} directly
Reservoir pressure	1557	-	"	[psi]	-	Not used. Instead, use above method to compute P_{wf} directly

2.3.4 Hydrocarbon Properties

Table 11 shows the default OPGEE inputs for fluid properties as well as the assumed OPGEE inputs for the Bakken case. It includes API gravity of the produced crudes, as well as typical Bakken gas composition, in mol% (equal to vol%).Of particular interest in Table 11 is the median composition of produced gas (normed so that percentages sum to 100%): the Bakken produced-gas composition is very heavy, and the fraction of CH_4 is approximately 50%. This finding implies the production of significant amounts of natural gas liquids (NGLs) from the

demethanizer unit in OPGEE (see processing practices discussion below). The detailed distributions of gas sample compositions are given in Table 12 and Figure 14. The pipeline specification gas composition produced by the OPGEE Bakken-default processing configuration after gas processing occurs (see discussion above) is given in Table 13.

Table 11. Produced fluid properties inputs

Data Input	OPGEE Default	Bakken Value	Freq. of Variation	Source	Notes
API gravity	30	Well API	Well-by-well	[10]	For wells without reported API gravity, mean across all wells of 41.90 deg. API is used.
Gas comp: N_2	2%	3.3%	No change	[10]	Median Bakken composition across all wells in reported test database.
Gas comp: CO_2	6%	0.7%	"	[10]	"
Gas comp: C_1	84%	50.8%	"	[10]	"
Gas comp: C_2	4%	21.1%	"	[10]	"
Gas comp: C_3	2%	14.6%	"	[10]	"
Gas comp: C_{4+}	1%	9.6%	"	[10]	"
Gas comp: H_2S	1%	0.0%	"	[10]	"

Table 12. Composition of gas for n = 710 gas samples from Bakken wells. All results in mol%.

	C_1	C_2	C_3	iC_4	nC_4	iC_5	nC_5	C_6	O_2/Ar	CO_2	N_2	H_2S
Mean	47.1	19.9	14.1	1.6	4.7	0.8	1.3	1.7	0.1	1.2	7.6	0.18
Median	49.2	20.5	14.1	1.5	4.5	0.8	1.1	1.4	0.0	0.6	3.2	0.00
Mean (norm to 100%)	47.0	19.8	14.0	1.6	4.7	0.8	1.3	1.7	0.1	1.2	7.5	0.2
Median (norm to 100%)	50.8	21.1	14.6	1.6	4.6	0.8	1.2	1.4	0.0	0.7	3.3	0.0
5%-ile	17.5	8.9	5.3	0.5	1.7	0.2	0.4	0.2	0.0	0.3	0.6	0.00
25%-ile	42.9	18.7	11.0	1.2	3.5	0.5	0.8	0.8	0.0	0.5	2.1	0.00
50%-ile	49.2	20.5	14.1	1.5	4.5	0.8	1.1	1.4	0.0	0.6	3.2	0.00
75%-ile	55.3	22.0	16.4	1.8	5.7	1.1	1.6	2.1	0.0	1.0	5.4	0.00
95%-ile	63.7	27.3	21.4	2.7	8.5	1.6	2.9	3.8	0.8	4.1	44.8	0.04

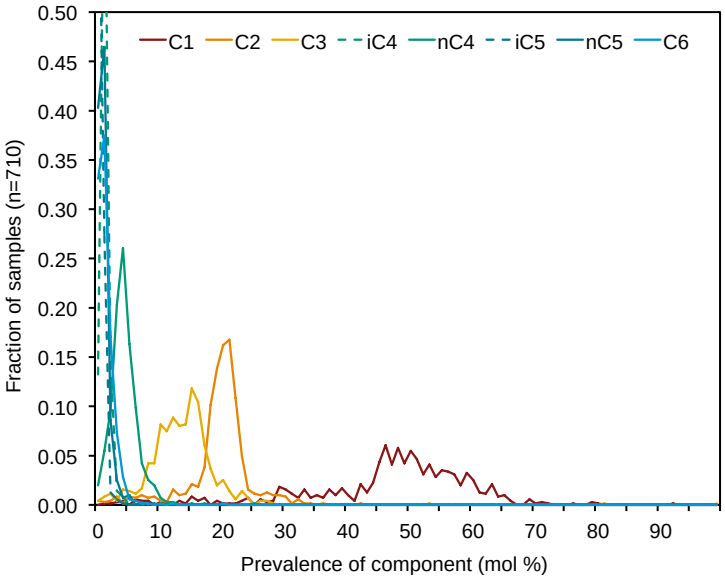

Figure 14. Gas composition distribution for hydrocarbon species C1 to C6. Non-hydrocarbon species are not included here, owing to very low prevalence.

Table 13. Pipeline gas composition (mol% or vol%) for default Bakken gas composition after assumed OPGEE gas processing scheme.

Data Input	OPGEE Default	Bakken Value	Freq. of Variation	Notes
Pipeline gas comp: N_2	2.4%	6.6%	No change	OPGEE "Gas Balance" sheet, Table 1.6. Result for average Bakken composition, post-gas-processing composition.
Pipeline gas comp: CO_2	0.0%	0.0%	"	"
Pipeline gas comp: C_1	97.2%	89.4%	"	"
Pipeline gas comp: C_2	0.5%	3.9%	"	"
Pipeline gas comp: C_3	0.0%	0.0%	"	"
Pipeline gas comp: C_{4+}	0.0%	0.0%	"	"
Pipeline gas comp: H_2S	0.0%	0.0%	"	"

2.3.5 Processing Practices

Processing practices for Bakken crude oil and natural gas are selected to be typical of applications in the Bakken formation. Separation of oil-water emulsions through heating is a common processing practice, and is used in the Bakken formation [43]. For this purpose, a gas-fired heater/treater is assumed to be used at all Bakken wells [43, pp. 33–35]. Temperatures reported in Bakken heater/treaters vary significantly [43, Appendix 5]. The high range of reported Bakken heater/treater temperatures aligns with the OPGEE default temperature (165°F), so we use the OPGEE default value. It is not clear how operator separation temperatures are chosen, so no rule set is used to assign temperatures to wells.

Further treatment of Bakken crude in a stabilization column is not expected to commonly occur in practice [43, p. 36], so we assume no use of a stabilization column in OPGEE.

The gas processing configuration is modeled generally after the Hess Inc. Tioga gas plant, the largest gas processing plant in the Bakken play (250,000 mcf per day of capacity) [44, 45]. The Tioga gas plant configuration includes acid gas removal, gas dehydration, and cryogenic gas fractionation to remove higher hydrocarbons. In our modeling, acid gas removal is modeled using the OPGEE default configuration of monoethanolamine (MEA) based amine acid gas scrubbing. Because Bakken gas tends to be sweet (low H_2S and CO_2 concentrations), MEA-based acid gas removal does not constitute a significant energy demand. Gas dehydration is assumed to occur with an OPGEE-default glycol dehydrator. Because the Bakken gas composition is very rich in higher hydrocarbons, fractionation is assumed to be applied to recover valuable liquefied petroleum gases (LPGs) and to lower the heating value of the gas to pipeline specifications. The OPGEE cryogenic demethanizer option is thus used, which is similar to the cryogenic separation technology actually applied at the Hess Tioga gas plant.

The flaring rate for each well is taken from the DMR production dataset (as reported above). The venting and leakage rate is set equal to the OPGEE default, owing to lack of information on these practices in the Bakken. No diluent is required for Bakken crude transport, nor is on-site non-integrated upgrading performed.

Table 14 shows the default OPGEE inputs for processing practices as well as the assumed OPGEE inputs for the Bakken case.

Table 14. Processing practices inputs

Data Input	OPGEE Default	Bakken Value	Freq. of Variation	Source	Notes
Heater/treater	0	1	No change	[43]	OPGEE defaults estimate heater/treater temperature of 165°F.
Stabilizer column	1	0	"	[43]	Bakken crude does not appear to be stabilized.
Application of AGR unit	1	1	"	[45]	Based on Tioga gas plant.
Gas dehydration unit	1	1	"	[45]	Based on Tioga gas plant.
Demethanizer unit	1	1	"	[45]	Based on Tioga gas plant, cryogenic fractionation.
Flaring-to-oil ratio	181.5	Well flaring rate	Monthly for each well	[1]	Each well reports flaring by month.
Venting-to-oil ratio	0	0	No change	[1]	All wells report venting of 0 mcf/month.
Vol. frac. of diluent	0	0	"	-[a]	Bakken crude is not diluted.
Non-integrated upgrader	0	0	"	-	Bakken crude is not upgraded.

[a] Symbol [-] indicates no information required.

2.3.6 Land Use Impacts

Land use impacts are modeled in OPGEE using two variables: crude ecosystem richness and field development intensity. The options for crude ecosystem richness correspond to various levels of carbon emissions possible upon disturbance of soil and standing biomass carbon. Low carbon richness represents arid or semi-arid grasslands, while high carbon richness is defined as heavily forested land. Moderate carbon richness is an intermediate classification.

The options for field development intensity relate to the amount of land disturbance per unit of oil produced. Example development intensities used to derive OPGEE intensities are from Yeh et al. [46] and range between dispersed natural gas drilling in conventional formations (low disturbance) to intensive thermal recovery drilling in California's Central Valley (high disturbance).

The carbon richness for the portion of North Dakota overlying the Bakken formation is chosen to be moderate, as the land is commonly used as productive agricultural land (e.g., not arid) while it is also not generally forested. The level of land disturbance is classified as low, owing to the use of multi-well pads with long laterals that allow contact with large reservoirs using small surface footprints (see Figure 15).

Table 15 shows the default OPGEE inputs for land use impacts as well as the assumed OPGEE inputs for the Bakken case.

Figure 15. Example of land disturbance due to oil drilling in the Bakken play. Image taken from north of Fort Berthold Reservation. Wellpads are cleared brown areas near roads.

Table 15. Land use impact inputs

Data Input	OPGEE Default	Bakken Value	Freq. of Variation	Notes
Ecosystem carbon richness: Low	0	0	No change	
Ecosystem carbon richness: Moderate	1	1	"	Farmland
Ecosystem carbon richness: High	0	0	"	
Field development intensity: Low	0	1	"	See Figure 15 above.
Field development intensity: Moderate	1	0	"	
Field development intensity: High	0	0	"	

2.3.7 Crude Oil Transport

Crude produced from the Bakken is generally trucked from on-site storage tanks to terminals for long-distance transport by pipeline and rail. There are currently 16 rail loading terminals in the Bakken region, along with three pipeline and refinery loading areas [47]. Given the approximate area of the North Dakota Bakken (of order 100 mi by 100 mi), evenly spaced terminals could ideally be placed on a grid, ~25 miles apart. We therefore conservatively estimate a trucking distance of 25 miles. Rail shipment began in August 2008, and before this time period all crude was refined locally, exported by pipeline, or trucked to Canadian pipelines. As of the end of 2013 [48], North Dakota had 515,000 bbl/day of pipeline capacity in three major export pipelines, 68,000 bbl/day of local refinery capacity, and rail loading capacity of 1,150,000 bbl/day. As these capacities in total (1.733 M bbl/day) exceed the output of the Bakken formation, not all modes are currently used to full capacity.

We estimate shipment breakdown using monthly data provided by the North Dakota Pipeline Authority (NDPA) [49]. For February 2012 to May 2014, the disposition and crude shipment by mode is reported directly by the NDPA as a fraction of total Williston Basin crude output. For months up to January of 2012, the NDPA estimates monthly rail shipment volumes (in most months with a high-low range), and year-end capacities for each mode are also computed by pipeline and rail terminal [48]. No information is available for the period prior to founding of the NDPA in early 2007.

The following method is used to compute disposition fractions:

- From February 2012 to May 2014, fractions of shipments are used directly as reported.
- From 2007 to January 2012, we assume that local refining is the preferred option. If production volumes exceed local refinery capacity (as has been the case since early 2008), then the remainder is assumed shipped by rail (as reported by NDPA) or pipeline (remainder). No truck transport of crude is assumed. These values are smoothed with a 3-month rolling average to remove large shifts that appear to be due to irregularities in the reported rail shipping data.
- Before 2007, all crude is assumed to have been refined locally (volumes are very small).

The resulting shares of Bakken crude transport over time are plotted in Figure 16.

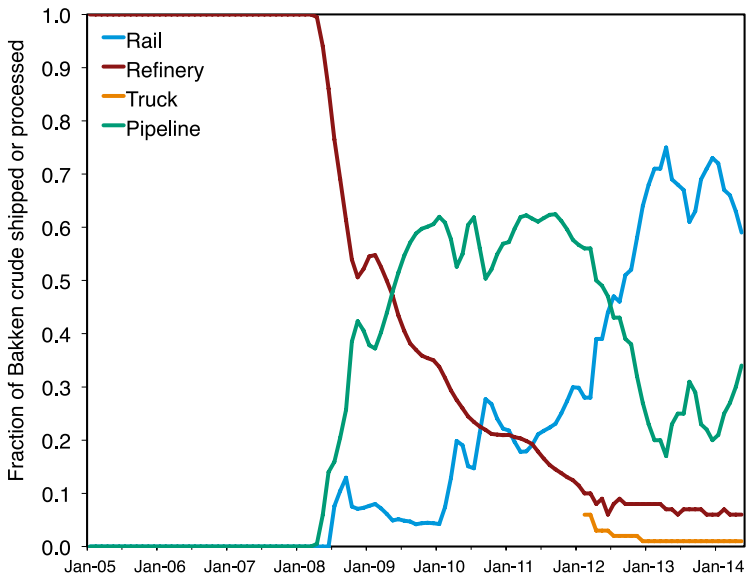

Figure 16. Fraction of crude shipped by indicated mode (pipeline, rail, or truck to Canadian pipeline) or locally processed (refinery).

The destinations for Bakken crude will vary over time because of seasonal demand, regional price differentials, and refineries' ability to take Bakken crude.

Recent rail destinations have been reported with volumetric offloading capacity [47]. We define four regions: Gulf coast, mid-continent, west coast, and east coast. Using these definitions, recent rail capacities were as follows:

- Gulf coast (Houston, TX; Port Arthur, TX; St. James, LA) = 400,000 bbl/day
- Mid-continent (Hayti, MO; Hennepin, IL; St. Louis, MO; Stroud, OK; Cushing, OK; Tulsa, OK) = 164,000 bbl/day
- West coast (Vancouver, WA; Bakersfield, CA; Anacortes, WA; Ferndale, WA; Portland, OR) = 265,000 bbl/day
- East coast (Albany, NY; Delaware City, DE; Saint John, NB) = 340,000 bbl/day

Representing these four regions by the largest volume off-take locations (Houston, Cushing, Vancouver/Portland, and Albany, respectively), we get estimated distances from Williston, ND, as follows [50]:

- Gulf coast: 1345 mi by shortest-path, 1585 mi by road
- Mid-continent: 911 mi by shortest-path, 1128 mi by road
- West coast: 917 mi by shortest-path, 1206 mi by road

- East coast: 1489 mi by shortest-path, 1851 mi by road

It is expected that road distances are a better proxy for rail distance than shortest-path distances. Weighting these distances by the volumetric capacity of each region gives a weighted average of 1512 mi. We therefore assume that crude travels 1500 mi by rail.

No information was found on final destinations of pipelined Bakken crude, as the crude first makes its way to regional hubs in the Cushing, OK, Chicago, IL, and Kansas City, MO, regions, after which the crudes may presumably be traded to a variety of consuming refineries around North America. Because such shipments are not reported in public datasets, we assume that the average distance of pipeline transport is identical to rail, i.e., 1500 mi.

Table 16 shows the default OPGEE inputs for crude transport as well as the assumed OPGEE inputs for the Bakken case.

Table 16. Crude oil transport inputs

Data Input	OPGEE Default	Bakken Value	Units	Freq. of Variation	Notes
Fraction transported: Ocean tanker	1	0	[bbl/bbl]	None	
Fraction transported: Barge	0	0	[bbl/bbl]	None	
Fraction transported: Pipeline	1	Var.	[bbl/bbl]	Monthly	
Fraction transported: Rail	0	Var.	[bbl/bbl]	Monthly	
Transport distance: Ocean tanker	5082	0	[mi]	None	One-way
Transport distance: Barge	500	0	[mi]	None	One-way
Transport distance: Pipeline	750	1500	[mi]	None	Assumed equal to rail distances
Transport distance: Rail	800	1500	[mi]	None	One-way

2.3.8 Small-Source Emissions

An additional "small source" emissions term is included in OPGEE to include all sources that are too small to be enumerated or modeled in detail (default = 0.5 g CO_2eq./MJ). We maintain this default value for the Bakken case, owing to lack of other information.

3 RESULTS

3.1 Production and Productivity Results

Input data for the productivity of each well in the dataset were analyzed to determine the characteristics of our population of wells. Because our population of modeled wells may differ slightly from other definitions of "Bakken wells," the total production rates, per-well productivities, and other production statistics might differ slightly from those seen elsewhere.

First, we show the amount of oil produced by the wells in our dataset for each month from 2006 to 2013 (see Figure 17). We note that production reached over $1x10^6$ bbl/day by the end of the dataset. By the end of 2013, nearly $8x10^5$ bbl/day were produced from wells with some flaring occurring. The fraction of oil produced from wells that flared a non-zero amount of gas increased over the time series, reaching ~75% by the end of 2013.

Next, we show the gas production over time (see Figure 18). We see that gas production reached over 1000 mmscf/day by the end of 2013, and that the flaring rate varied between 20% and 50% of gas produced over the time series, with the trend in the most recent months being toward reduced flaring.

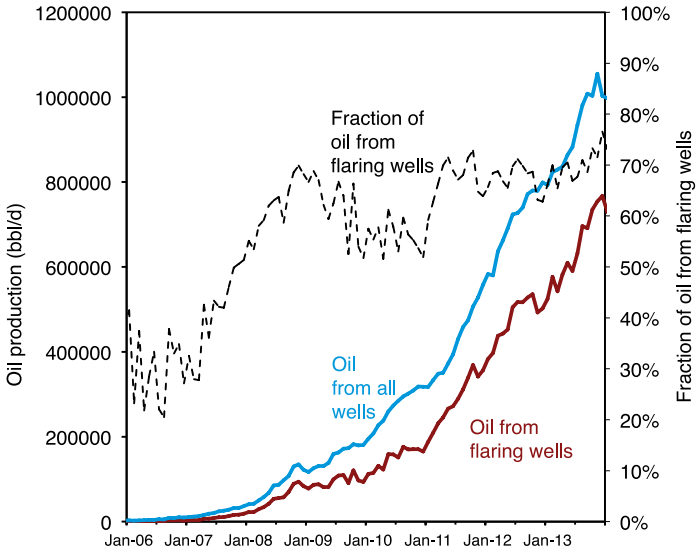

Figure 17. Oil production over time from all wells in dataset. Oil from flaring wells represents oil produced from wells where the flaring rate is > 0 scf/bbl.

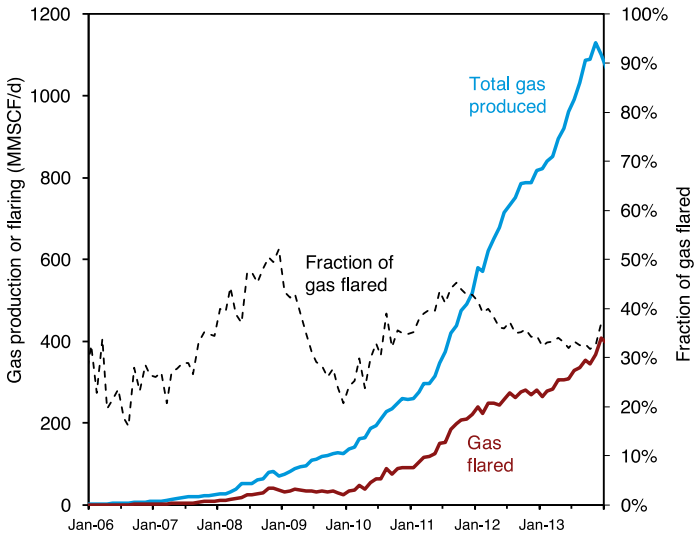

Figure 18. Gas production over time from all wells in dataset. Gas flared is the amount of gas reported as flared in DMR datasets. Gas consumed on site ("lease fuel") is not included in flared gas.

Figure 19 shows the distribution of per-well productivities across all months in the dataset (January 2005 to April 2014). Across the 7,271 wells in the dataset and 112 months of observations, a total of 211,725 observations of per-well daily productivity were generated. Figure 20 shows a time series plot of these results for 2006–2013, inclusive. The shaded region bounds the inter-quartile range (25th to 75th percentile), while the dotted curves bound the range in which 90% of observations fell (5th to 95th percentile). Both median and mean are presented as measures of central tendency. We can see that this distribution is skewed, with the mean value approaching the 75th percentile in many months. We see that per-well productivity increased in the early years of Bakken production, and has decreased slightly since reaching a peak of about 200 bbl/well-day in mid-2008. Productivities hovered around 150 bbl/well-day at the end of the data series.

We next generated similar results for two ratios of interest: WOR and GOR. Because these values are ratios, some wells with a month of very small (near-zero) reported oil production will yield an outlier value many orders of magnitude larger than typical values. For this reason, the figures below present mean results computed after removing the largest 0.01% of observations. Median and percentile computations are unaffected by such outliers, and so are computed using the full dataset.

Figure 21 and Figure 22 show analogous results for the WOR, measured in bbl of produced water per bbl of crude plus lease condensate produced. Note that all DMR statistics reported above and elsewhere in this report for "crude" oil production are for crude oil plus lease condensate. Again, our time series shows a skewed distribution, with production-weighted mean observations approaching the 75th percentile. The WOR declined in early years of production, but has increased since mid-2009 to about 1 bbl/bbl on a production-weighted mean basis at the end of 2013.

Figure 23 and Figure 24 show analogous results for the GOR, measured in scf of produced raw gas per bbl of crude + lease condensate. This distribution is somewhat less skewed than the WOR distribution, with the production-weighted mean value resting in most years between the median and 75th percentile. The GOR has been relatively constant over the time period of analysis, with 90% of observations (5th to 95th percentile) falling between 250 and 2500 scf/bbl, and production-weighted mean values of around 1000 scf/bbl in most months.

Tabular results for productivity, WOR, and GOR are presented in Table 17, Table 18, and Table 19, respectively. Because the small number of months with outlier effects noted above are not material in computing yearly averages, the production-weighted average WOR and GOR statistics are computed for all data points in the year of interest.

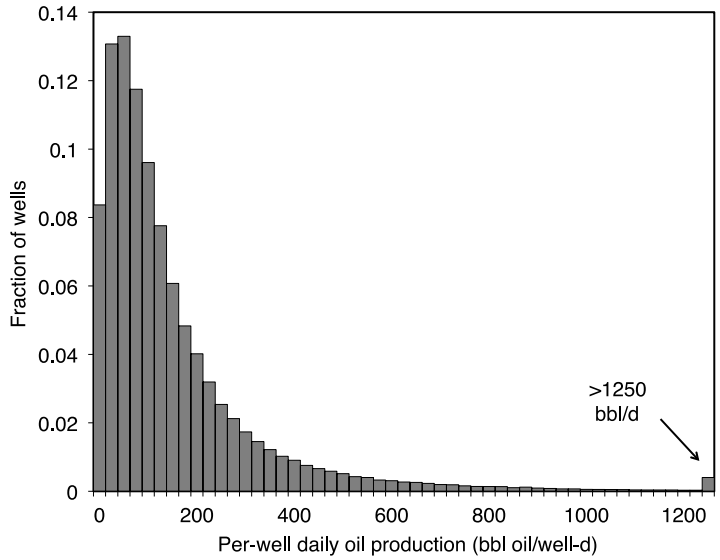

Figure 19. Distribution of oil well productivity, all years. n = 211,725 observations. Units: bbl per well per day.

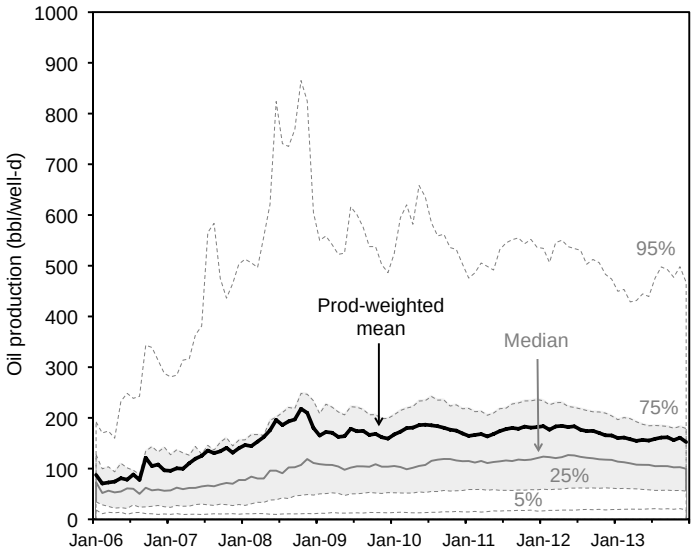

Figure 20. Distribution of oil well productivity over time, January 2006–December 2013. Units: bbl per well per day.

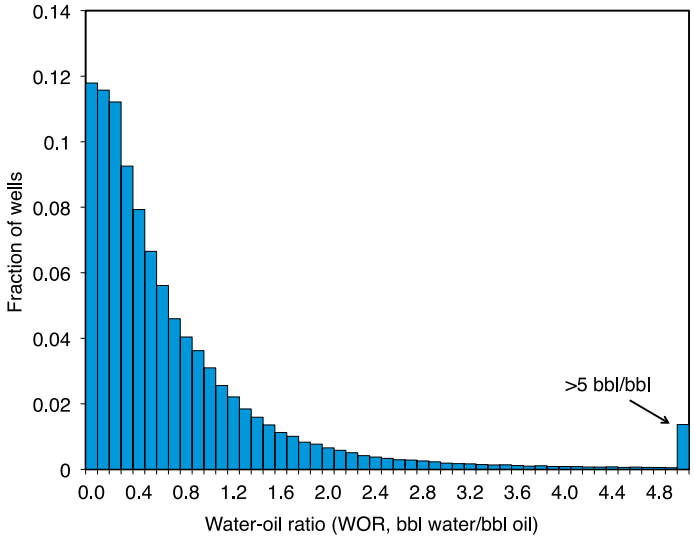

Figure 21. Distribution of water-oil-ratio, all years. n = 211,725 observations. Units: bbl water per bbl oil.

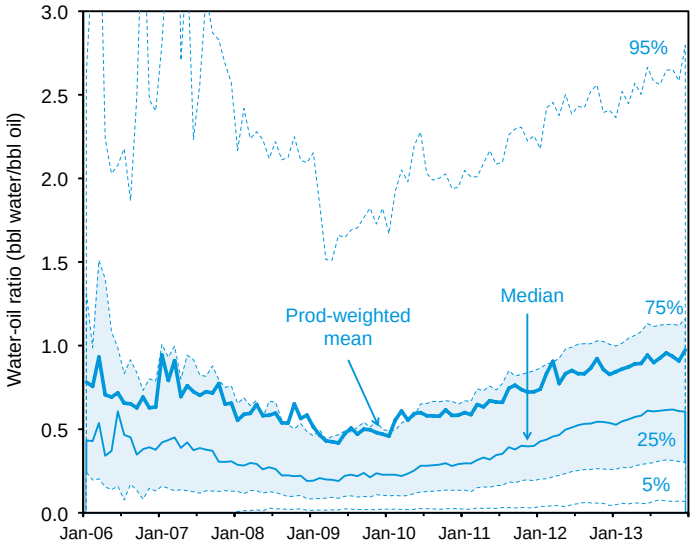

Figure 22. Distribution of water-oil ratio over time, January 2006–December 2013. Units: bbl of water per bbl of oil.

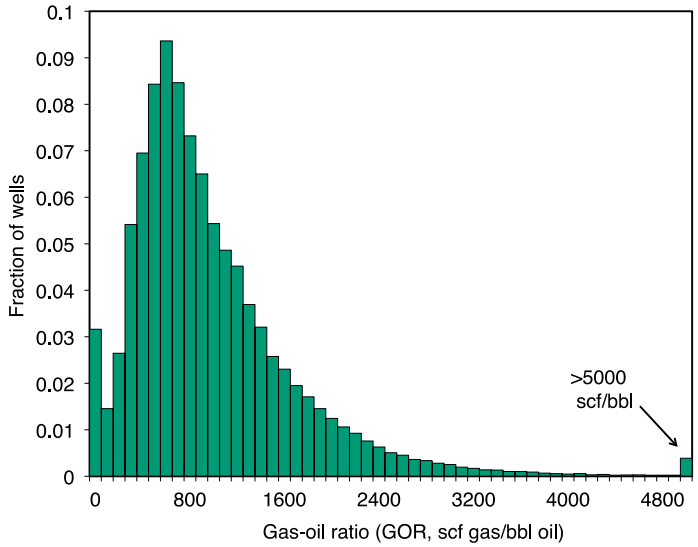

Figure 23. Distribution of gas-oil-ratio, all years. n = 211,725 observations. Units: scf gas per bbl.

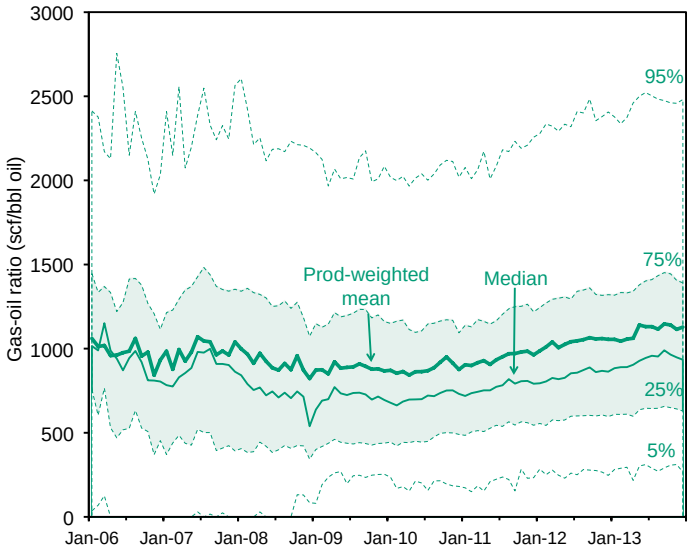

Figure 24. Distribution of gas-oil-ratio over time, January 2006–December 2013. Units: scf gas per bbl.

Table 17. Well productivity summary statistics. Only observations for complete years are computed (removing Jan.–April 2014). Observations for 2005 are not recorded because of the small number of wells operating in this time period.

	2006	2007	2008	2009	2010	2011	2012	2013	All Years	Units
Avg. number of operational wells	61.6	178.7	458.8	920.1	1505.9	2418.0	4016.0	5807.7	-	[num wells]
Total crude + condensate production	5703	22457	85147	154410	268914	422724	706261	917732	-	[bbl/day]
Mean per-well prod.	93	126	186	168	179	175	176	158	168	[bbl/well-day]
Median per-well prod. (50%)	57	68	97	104	110	116	121	106	111	[bbl/well-day]
5%-ile	11	10	11	13	14	16	19	20	17	[bbl/well-day]
25%-ile	26	27	41	51	54	58	61	58	57	[bbl/well-day]
75%-ile	120	144	212	211	227	222	218	188	206	[bbl/well-day]
95%-ile	280	435	715	548	570	525	515	464	511	[bbl/well-day]

Table 18. Water-oil ratio summary statistics. Only observations for complete years are computed (removing Jan.–April 2014). Observations for 2005 are not recorded because of the small number of wells operating in this time period.

	2006	2007	2008	2009	2010	2011	2012	2013	All Years	Units
Mean	0.774	0.973	0.637	0.519	0.651	0.803	1.011	1.041	0.912	[bbl/bbl]
Prod-weighted Mean	0.353	0.298	0.296	0.298	0.453	0.570	0.685	0.718	0.614	[bbl/bbl]
Median (50%)	0.408	0.366	0.237	0.216	0.266	0.356	0.51	0.59	0.456	[bbl/bbl]
5%-ile	0.0000	0.0000	0.0180	0.0184	0.0223	0.0278	0.0481	0.0628	0.035	[bbl/bbl]
25%-ile	0.1465	0.1309	0.1078	0.0944	0.1197	0.1657	0.2416	0.2931	0.203	[bbl/bbl]
75%-ile	0.9191	0.8474	0.5741	0.4970	0.6196	0.7793	0.9790	1.0949	0.935	[bbl/bbl]
95%-ile	2.5824	2.8884	2.2154	1.7254	2.0187	2.1651	2.4322	2.5961	2.400	[bbl/bbl]

Table 19. Gas-oil ratio summary statistics. Only observations for complete years are computed (removing Jan.–April 2014). Observations for 2005 are not recorded because of the small number of wells operating in this time period.

	2006	2007	2008	2009	2010	2011	2012	2013	All Years	Units
Mean	1218	1072	927	903	949	984	1223	1322	1166	[scf/bbl]
Prod-weighted mean	874	782	630	688	752	887	999	1062	944	[scf/bbl]
Median (50%)	906	896	713	717	714	778	849	934	847	[scf/bbl]
5%-ile	0	0	11	230	193	205	263	288	240	[scf/bbl]
25%-ile	508	429	402	434	464	536	588	632	562	[scf/bbl]
75%-ile	1315	1359	1250	1191	1143	1203	1313	1392	1302	[scf/bbl]
95%-ile	2348	2376	2231	2073	2038	2156	2370	2455	2327	[scf/bbl]

3.2 Drilling Results

The calculated diesel fuel use for drilling-rig top drive (torque applied to top of drill string) and mud pump circulation (pumping work to overcome friction, nozzle loss, and mud motor) are shown in Figure 25 and Figure 26, respectively. The resulting diesel fuel use for fracturing pump work (pumping work to force fluids into wellbore) is shown in Figure 27. These amounts of drilling energy are input into the OPGEE model (as noted above) and amortized over the life of the well using the modeled EUR (as noted above). The resulting input distributions for energy use in drilling as a function of time are plotted in Figure 28 and are presented in Table 20 for all years.

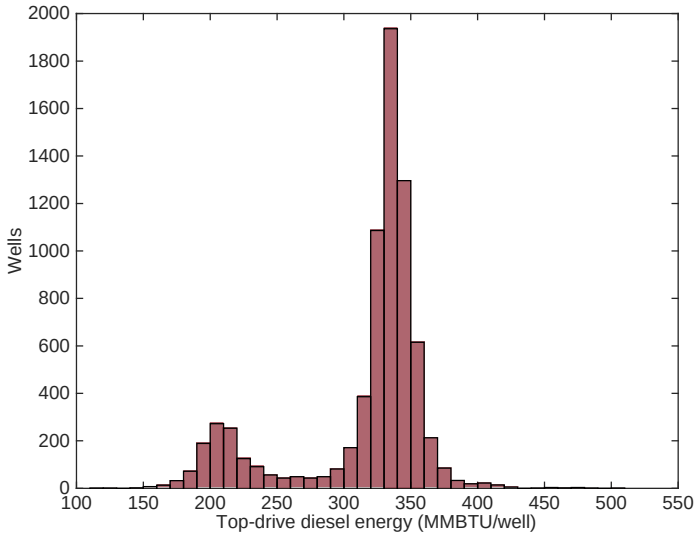

Figure 25. Distribution of diesel use for powering drilling top drive, using computation method described above.

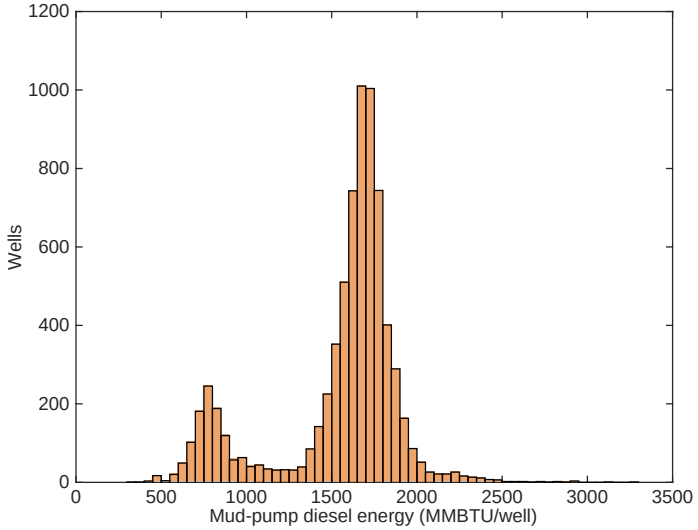

Figure 26. Distribution of fuel use by mud pump to drive drilling mud circulation.

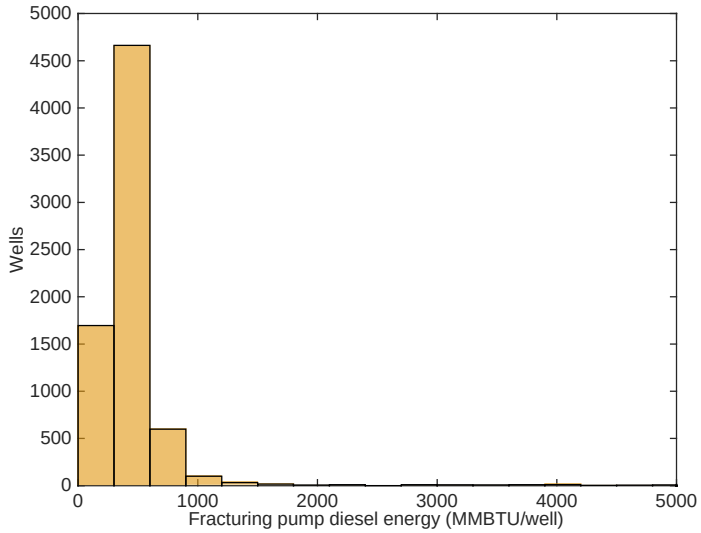

Figure 27. Distribution of fuel use by fracturing-fluid pump during hydraulic fracturing.

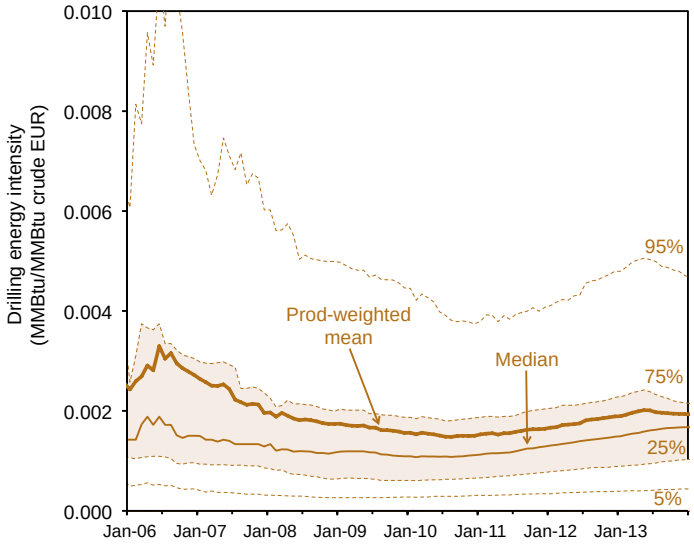

Figure 28. Drilling energy intensity as a function of time.

Table 20. Energy intensity of drilling and hydraulic fracturing, all wells in dataset. Unit: Btu of diesel used in drilling rig (direct energy) per mmBtu of estimated ultimate recovery (EUR) of crude + condensate.

	All Years	Units
Mean	1922	[Btu/mmBtu]
Median	1685	[Btu/mmBtu]
5%-ile	454	[Btu/mmBtu]
25%-ile	1049	[Btu/mmBtu]
75%-ile	2107	[Btu/mmBtu]
95%-ile	4592	[Btu/mmBtu]

3.3 Monthly Energy Intensity Results

Table 21 shows calculated natural gas consumption per mmBtu of crude oil plus lease condensate produced. The results for each month are plotted as a function of time in Figure 29, showing distribution percentiles and mean and median consumption. We see that the use of fuel has remained relatively constant over the life of the play.

Table 22 shows calculated diesel consumption per mmBtu of crude oil plus lease condensate produced. The diesel consumption as a function of time is plotted in Figure 30.

Table 23 shows calculated electricity consumption per mmBtu of crude oil plus lease condensate produced. Natural gas is used on site for pumping, processing, and heating. Diesel is used for drilling and for on-site electricity generation. Electricity is used for pumping, cooling, and chilling. The electricity consumption per unit of crude plus condensate produced is shown in Figure 31as a function of time.

All of these factors are for monthly production, e.g., electricity consumed in a given month per mmBtu of crude plus lease condensate produced in that month. Only the above drilling results are averaged over the life of the well. We see that natural gas consumption (in 2013) amounted to perhaps 1.3% of the energy content of crude (~13,000 Btu/mmBtu), diesel consumption amounted to less than 0.2% of the energy content of produced crude (~1,800 Btu/mmBtu), and electricity consumption was very small (~50 Btu/mmBtu). Thus, total direct consumption of fuels for productive purposes reached (on average) 1.5% of the energy content of the produced crude oil in 2013.

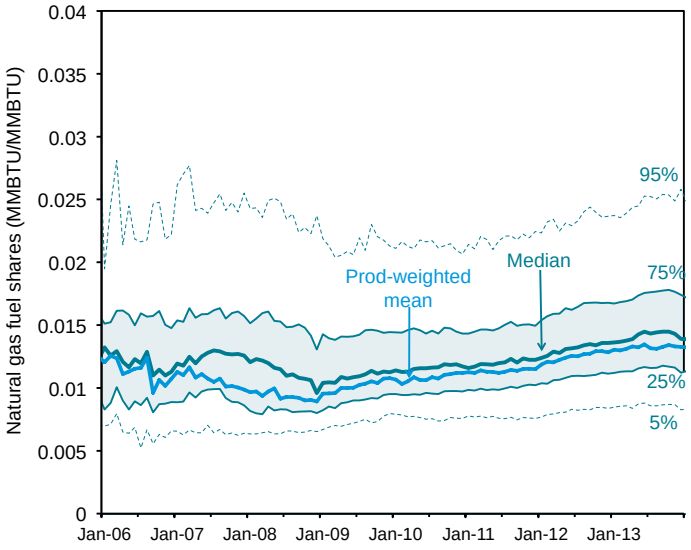

Figure 29. Distribution of natural gas consumption intensity over time (mmBtu natural gas consumed/mmBtu of crude oil).

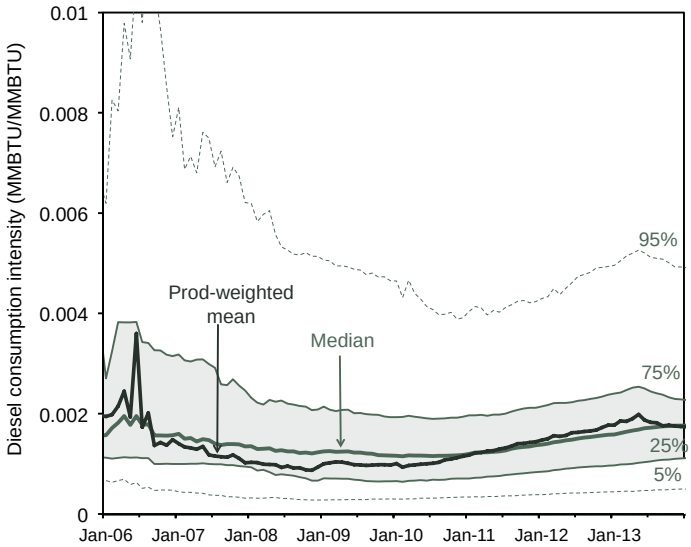

Figure 30. Distribution of diesel consumption intensity over time (mmBtu diesel consumed/mmBtu of crude oil).

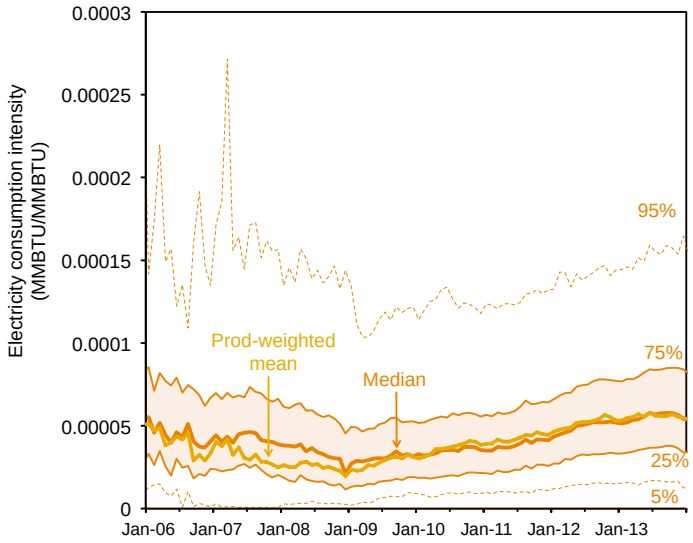

Figure 31. Distribution of electricity consumption intensity over time (mmBtu electricity consumed/mmBtu crude oil)

Table 21. Natural gas consumption per mmBtu of oil (crude + lease condensate) produced

	2006	2007	2008	2009	2010	2011	2012	2013	All	Units
Average	13510	14763	12871	12553	13386	13660	16282	17476	15683	Btu/mmBtu
Prod-weighted average	10966	10487	9259	10202	10844	11366	12516	13229	12140	Btu/mmBtu
Median	11756	12574	10896	10983	11635	12046	13189	14154	13024	Btu/mmBtu
5%-ile	6287	6349	6473	7184	7601	7635	8187	8564	7784	Btu/mmBtu
25%-ile	8717	9328	8144	9035	9593	10005	10842	11478	10491	Btu/mmBtu
75%-ile	15660	15956	14897	14306	14514	14845	16375	17404	16280	Btu/mmBtu
95%-ile	23040	25143	23544	21482	21309	21866	23456	24817	23631	Btu/mmBtu

Table 22. Diesel consumption per mmBtu of oil (crude + lease condensate) produced

	2006	2007	2008	2009	2010	2011	2012	2013	All	Units
Average	2962	2377	1892	1714	1591	1674	1921	2091	1910	Btu/mmBtu
Prod-weighted average	1771	1179	934	993	1038	1330	1622	1821	1520	Btu/mmBtu
Median	1678	1408	1257	1213	1164	1283	1491	1716	1491	Btu/mmBtu
5%-ile	481	372	294	291	316	359	417	470	388	Btu/mmBtu
25%-ile	1085	982	763	674	681	776	918	1043	894	Btu/mmBtu
75%-ile	3273	2914	2166	1996	1924	2032	2258	2411	2237	Btu/mmBtu
95%-ile	23040	25143	23544	21482	21309	21866	23456	24817	23631	Btu/mmBtu

Table 23. Electricity consumption per mmBtu of oil (crude + lease condensate) produced

	2006	2007	2008	2009	2010	2011	2012	2013	All	Units
Average	60	71	51	45	53	59	90	90	77	Btu/mmBtu
Prod-weighted average	37	31	25	28	37	43	52	56	48	Btu/mmBtu
Median flaring rate (flaring wells only)	43	42	32	31	35	39	50	55	47	Btu/mmBtu
5%-ile	4	1	3	6	9	10	14	16	11	Btu/mmBtu
25%-ile	24	23	15	16	20	24	31	36	28	Btu/mmBtu
75%-ile	71	68	56	51	55	61	74	82	73	Btu/mmBtu
95%-ile	162	168	144	116	124	127	141	154	143	Btu/mmBtu

3.4 Flaring Intensity Results

The amount of natural gas flared from the wells studied here has risen in lockstep with the amount of oil produced. Figure 32 shows the increase in oil produced (energy content, measured as mmBtu/day) and natural gas flared (energy content, measured as mmBtu/day) on a logarithmic scale from 2006 to 2013. As can be seen, both of these quantities have risen by about three orders of magnitude (1000x) over the time period. However, the ratio has stayed fairly constant, with the energy content of the flared gas ranging from 5% to 15% of the energy content of the produced crude oil. At the end of the study period in late 2013, the energy content of flared gas was approximately 13% of the energy content of produced oil. Overall, the volume of flared gas reached about 400 mmscf/day by the end of 2013 (Figure 33, right axis).

The intensity of gas flaring per unit of oil produced can be measured using two metrics. First, we can measure gas flaring rates from wells that flare, by dividing the volume of flared gas by the oil produced by those wells (scf/bbl). Second, we can divide the total volume of gas flared by the oil produced from all wells, flaring and non-flaring (scf/bbl). Both of these ratios are shown over time in Figure 33.

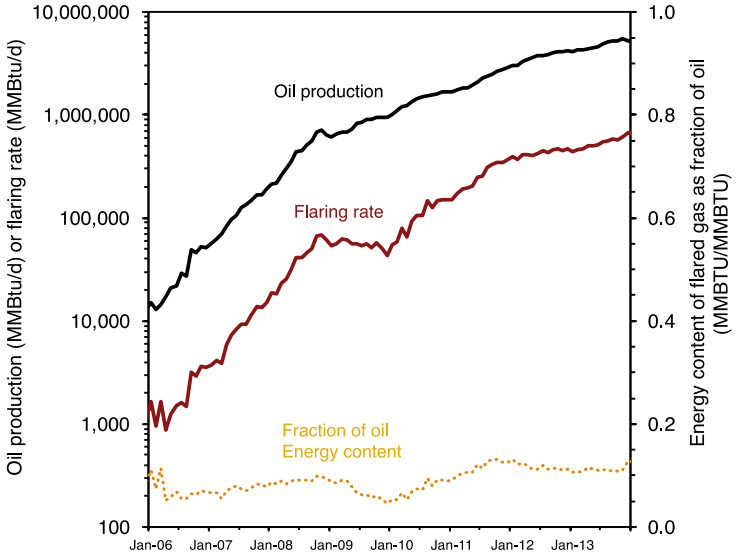

Figure 32. Left axis: Amounts of oil produced and gas flared, in mmBtu/day (note logarithmic scale). Right axis: Fractional energy content of flared gas compared to oil energy content (yellow dashed line).

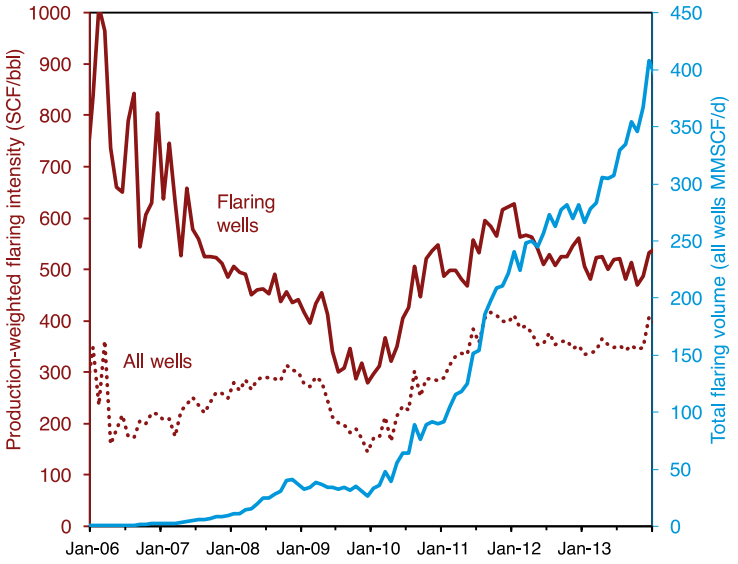

Figure 33. Left axis: Flaring intensity per bbl of crude + condensate for wells that flare and for all wells (flaring and non-flaring). Right axis: Total flaring volume (blue line).

The distribution of flaring rates, both on a normalized basis and on an absolute basis, is skewed, with the mean flaring rate higher than the median (sometimes significantly so). Figure 34 shows the per-bbl flaring rate distribution as a function of time. The shaded region is the interquartile range (25^{th} to 75^{th} percentile), and the dotted curves outline the range encompassing 90% of the observations (5^{th} to 95^{th} percentile). We see that in recent years, the production-

weighted mean flaring intensity (measured in scf/bbl for flaring wells only) is significantly higher than the median flaring intensity. Figure 35 shows a similar time series but for the absolute flaring volumes per well (mcf/well-day). Again, we see that the mean flaring volume is significantly higher than the median, in this case near the 75th percentile.

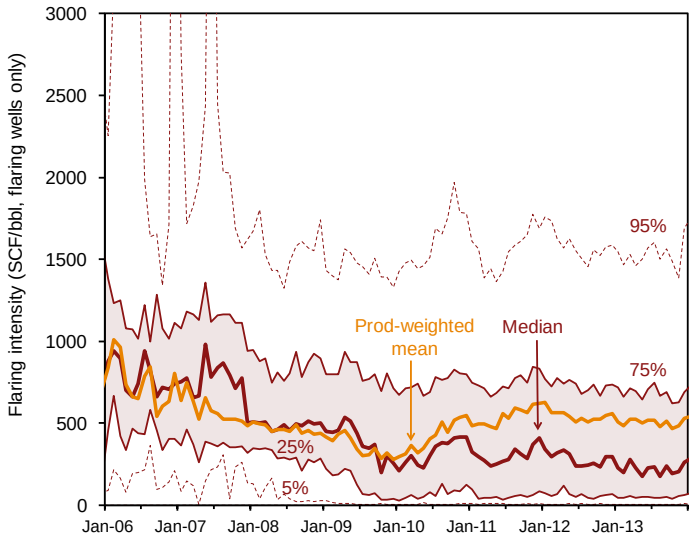

Figure 34. Distribution of per-bbl flaring intensity for flaring wells (scf/bbl crude + condensate) over time. These are monthly reported operational flaring rates, which do not include flowback flaring.

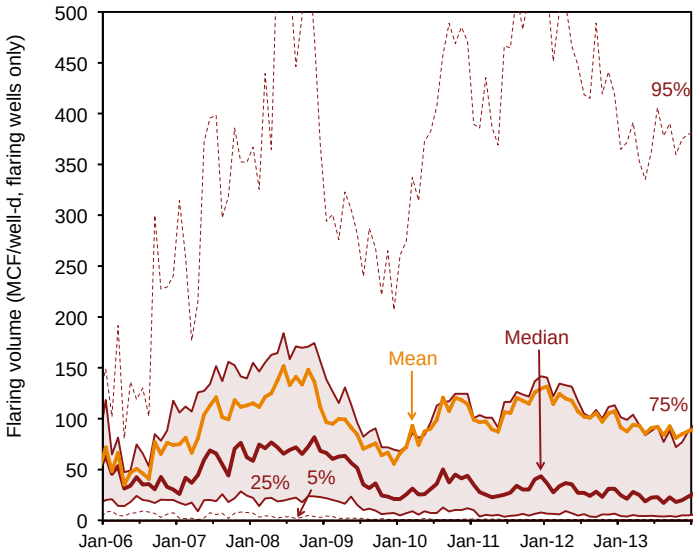

Figure 35. Distribution of per-well flaring intensity for flaring wells (mcf/well-day) over time. These are monthly reported operational flaring rates, which do not include flowback flaring.

The flaring intensity is not evenly distributed across wells of different productivities (see Figure 36). We divided each well-month observation into four flaring classes:

- Non-flaring wells, which had a flaring rate of exactly 0 scf/bbl in the month of observation;
- Low-flaring wells, which had a flaring rate between 0 and 100 scf/bbl in the month of observation;
- Medium-flaring wells, which had a flaring rate between 100 and 1000 scf/bbl in the month of observation; and
- High-flaring wells, which had a flaring rate of over 1000 scf/bbl in the month of observation.

In Figure 36, we plot the cumulative fraction of wells for each class that have a given per-well oil productivity. We can see that the high-flaring wells are significantly more productive than the non-flaring wells. 80% of non-flaring wells produced less than 200 bbl/day of crude oil, while 80% of high-flaring wells produced less than 400 bbl/day of crude oil. This increase in cumulative-share productivity holds across all flaring classes.

The efficiency of flaring is a function of both the flaring rate at a given well and the wind speed in a given month. The relationship governing flare efficiency is a reasonably complex empirical relationship requiring wind speeds and flare tip exit velocities (see OPGEE documentation [33] for more information). By computing the efficiency of methane destruction for each well-month observation using OPGEE's flaring module and local weather data on wind speed distributions, we can plot the distribution of flaring efficiencies over time (Figure 37). We see that the lowest efficiency range (5^{th} percentile) drops over time, but the volume-weighted mean destruction efficiency stays virtually stable over the study time period. This is because in any given month, most of the flaring comes from large flares which have quite high destruction efficiencies.

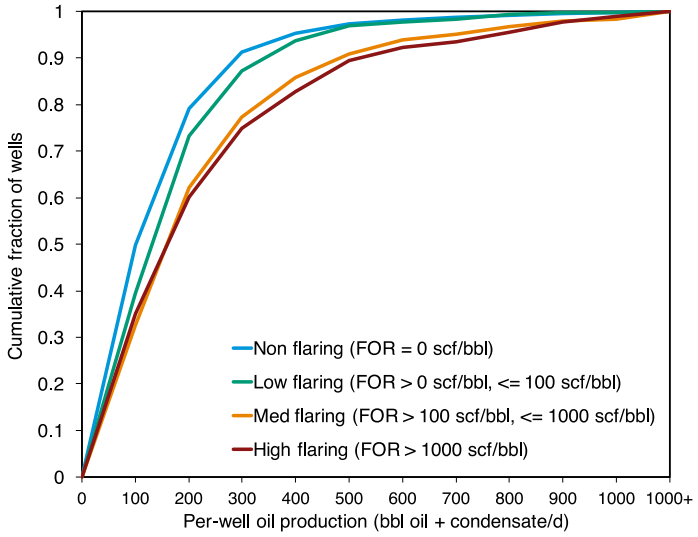

Figure 36. Cumulative distributions for well productivity for four flaring-intensity bins.

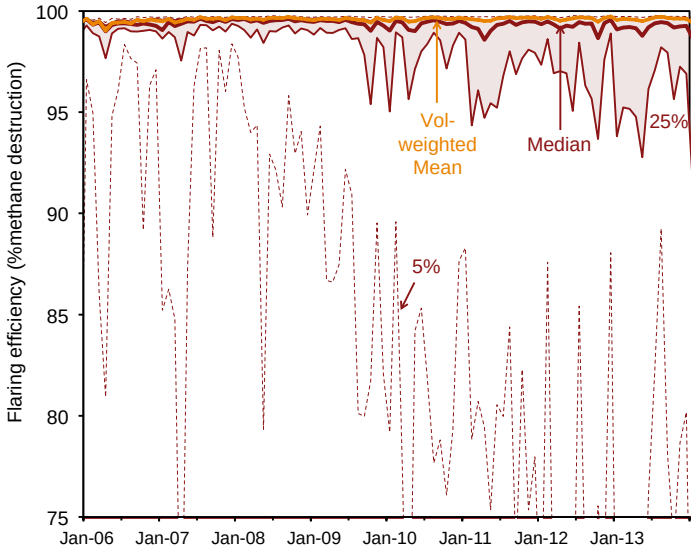

Figure 37. Flare methane destruction efficiency over time, computed on a per-well basis. Weighted mean is computed on a flare-volume weighted basis to account for different destruction efficiencies in small vs. large flares.

Flaring results are summarized numerically in Tables 24–26. Table 24 presents summary properties, including numbers of flaring wells and measures of flaring distributions for flaring wells only and for non-flaring wells. Table 25 presents results for the distribution of the absolute per-well volume flaring rate. Table 26 presents results for the methane destruction efficiency.

We note that the production-weighted mean flaring rate for wells that flare has hovered around 500 scf/bbl in recent years. At a heating value of 1500 Btu LHV per scf, this equals 0.75 mmBtu per bbl of crude. Given the OPGEE default energy density for 42 deg. API crude oil of 5.22 mmBtu per bbl of crude, the energy content of flared gas equals over 14% of the energy content of the crude.

Table 24. Flaring summary properties. Only observations for complete years are computed (removing Jan.–April 2014), and observations for 2005 are not recorded because of the small number of wells operating in this time period.

	2006	2007	2008	2009	2010	2011	2012	2013	Units
Avg. num.of wells flaring	20.3	52.1	188.3	419.8	650.2	1437.9	2361.9	3665.6	[num wells]
Avg. num. of wells not flaring	41.3	126.6	269.8	499.3	854.8	979.1	1653.1	2141.1	[num wells]
Fraction of oil from flaring wells	31%	44%	64%	61%	56%	67%	67%	70%	[%]
Mean flaring rate (flaring wells only)	1409	996	649	534	537	526	693	512	[scf/bbl]
Prod-weighted mean flaring rate (flaring wells only)	700	544	457	351	431	551	545	504	[scf/bbl]
Median flaring rate (flaring wells only)	742	733	488	399	347	314	282	218	[scf/bbl]
5%-ile	108	128	31	7	6	9	6	7	[scf/bbl]
25%-ile	427	355	296	81	64	55	61	49	[scf/bbl]
75%-ile	1177	1126	868	800	756	754	727	675	[scf/bbl]
95%-ile	3145	1989	1558	1448	1627	1576	1585	1532	[scf/bbl]
Mean flaring rate (all wells)	463	290	267	244	232	313	407	323	[scf/bbl]
Prod-weighted mean flaring rate (all wells)	215	238	292	216	241	371	367	353	[scf/bbl]

Table 25. Absolute flaring volume per well per day (flaring wells only)

	2006	2007	2008	2009	2010	2011	2012	2013	All Years	Units
Mean	60.4	102.5	131.8	79.2	99.6	109.2	109.7	88.3	98.8	[mcf/well-day]
Median	34.1	19.3	70.7	40.1	35.7	30.6	29.5	21.6	27.9	[mcf/well-day]
5%-ile	3.2	2.0	3.2	1.6	0.9	0.9	0.7	0.7	0.8	[mcf/well-day]
25%-ile	19.5	19.3	20.6	10.5	8.4	5.3	5.7	4.3	5.5	[mcf/well-day]
75%-ile	73.7	136.4	165.5	97.7	102.6	117.3	116.1	87.2	103.0	[mcf/well-day]
95%-ile	181.4	360.8	482.3	272.2	414.7	472.1	458.7	373.8	414.7	[mcf/well-day]

Table 26. Estimated flare methane destruction efficiency [%]

	2006	2007	2008	2009	2010	2011	2012	2013	All Years
Vol-weighted mean	99.49	99.60	99.63	99.58	99.62	99.63	99.63	99.61	99.62
Median	99.33	99.03	99.53	99.43	99.41	99.35	99.35	99.25	99.33
5%-ile	92.24	88.92	92.83	85.54	79.57	79.25	73.51	73.59	75.84
25%-ile	99.00	99.03	99.02	98.58	98.06	96.78	97.08	96.31	97.08
75%-ile	99.55	99.65	99.66	99.62	99.63	99.64	99.64	99.61	99.63
95%-ile	99.67	99.72	99.74	99.72	99.74	99.74	99.75	99.74	99.74

3.5 Co-Product Production Results

Significant amounts of energy products are co-produced along with oil in the Bakken formation. While "oil" is defined by DMR as crude + lease condensate, natural gas production lines carry away a significant amount of energy in the form of liquids-rich gas.

Bakken gas is very liquids-rich (see discussion on gas composition above). The gas contains, on average, less than 50% mol fraction methane, and about 2/3 of the energy content of the raw, unprocessed gas is contained in non-methane or condensable species. As noted above, we do not alter the OPGEE gas processing scheme from its default configuration. This means that we assume that NGLs are removed from the gas before it is consumed on site for fueling process equipment. Using values for 2013 in Table 27 and Table 28, we see that pipeline-specification natural gas exports (on a production-weighted average basis) amounted to about 5% of the energy content of the oil (50,000 Btu/mmBtu), while NGL exports amounted to nearly 14% of the energy content of the oil (137,000 Btu/mmBtu). The lowest-producing wells in terms of natural gas are found to have a natural gas deficit, in which the processing needs on site (heater/treaters, etc.) are larger than the gas produced (-1% balance for 5th percentile wells).

Table 27. Natural gas net exports per mmBtu of oil (crude + lease condensate) produced. (+) represents exports, (-) represents net imports.

	2006	2007	2008	2009	2010	2011	2012	2013	All years	Units
Average	54406	55286	46245	46096	50391	46070	56663	72216	59291	Btu/mmBtu
Prod-weighted average	48157	38352	20835	31330	34136	34373	43831	50008	41923	Btu/mmBtu
50% (median)	34808	34806	24017	29142	34253	35109	40719	45434	39601	Btu/mmBtu
95%-ile	168461	166224	165696	152313	145995	148894	171930	178354	167758	Btu/mmBtu
75%-ile	88603	92732	78258	72615	69631	67186	78730	86714	78972	Btu/mmBtu
25%-ile	-5895	-5676	-6216	-2400	5676	-4634	2967	9997	3243	Btu/mmBtu
5%-ile	-10741	-10707	-9397	-9061	-9950	-11073	-11551	-11587	-11167	Btu/mmBtu

Table 28. Natural gas liquid (NGL) net exports per mmBtu of oil (crude + lease condensate) produced

	2006	2007	2008	2009	2010	2011	2012	2013	All years	Units
Average	147063	151504	128749	127778	138451	130027	157536	192396	161759	Btu/mmBtu
Prod-weighted average	128769	107367	68340	92151	99317	100907	122991	137331	118235	Btu/mmBtu
50% (median)	100394	103218	77362	88284	99904	103476	117220	129339	114717	Btu/mmBtu
95%-ile	405314	397895	393724	361999	351536	356900	408495	423306	399334	Btu/mmBtu
75%-ile	224055	231509	200690	186267	180017	173999	201517	220107	202147	Btu/mmBtu
25%-ile	7579	7724	7545	21631	39043	16840	37838	53793	37455	Btu/mmBtu
5%-ile	7408	6946	6851	7443	7408	7373	7440	7472	7424	Btu/mmBtu

4 INCORPORATION OF DATA INTO GREET MODEL

The resulting information from the OPGEE model, as well as some raw inputs from above, were included in the GREET model to assess the GHG intensity of Bakken crude oil production. Methods for incorporating these results into GREET are described below.

4.1 Parametric Assumptions of Shale Oil Production in Bakken for GREET Incorporation

To model the greenhouse gas emissions (GHG) associated with shale oil production in Bakken with the GREET model, process fuel consumption by fuel type, the flaring intensity of produced gas, flaring efficiency, fugitive produced gas emissions, and chemical composition of produced gas are required parametric assumptions. In GREET, we treat the NG and NGL that are exported for sales as co-products for shale oil production. In addition, we applied the energy-based allocation method to allocate the process fuel consumption and emission burdens for shale oil by assuming that the utility of the energy embedded in oil, NG, and NGL is the same for their respective end users. There is no universally mandated co-product allocation method. Other co-product allocation methods, for example, market value-based allocation, could be used by burdening more of the process energy consumption and emissions to the energy products with higher market values.

From 2006 to 2013, there was no clear trend for the process fuel consumption intensities or flaring intensities, as shown in Table 21 to Table 24. Therefore, we combined the eight years' data to represent the operational performances of shale oil production in the Bakken. Table 29 summarizes the recovery energy efficiency, process energy use by fuel type, the flaring intensity, the fugitive intensity, water use, oil API gravity, GOR, and the O/T ratio for shale oil production in Bakken from 2006 to 2013. In addition, such parameters for flaring wells and non-flaring wells are presented separately in Table 30 and Table 31, respectively, which can be indicative of the difference in GHG emission implications of wells that flared and those that didn't.

Table 29. Summary of energy use and water use intensities associated with shale oil production in Bakken, 2006–2013, using energy allocation method, except as noted

	Recovery Energy Efficiency[a]	NG Use (Btu/mmBtu of oil)	Diesel Use (Btu/mmBtu of oil)	Electricity Use (Btu/mmBtu of oil)	Operational Flaring Intensity (SCF/mmBtu of oil)	Flowback Flaring Intensity (SCF/mmBtu of oil)	Fugitive Intensity (SCF/mmBtu of oil)	Water Use[c] (gal/gal of oil)	GOR[c] (SCF/bbl of oil)	O/T Ratio
Weighted average[b]	98.8%	10,443	1,308	41	55	0.07	6	0.22	1,167	0.86
1%-ile	96.8%	6,171	221	2	0	0.00	4	0.04	0	0.54
10%-ile	98.3%	8,377	442	15	0	0.01	5	0.10	360	0.69
25%-ile	98.6%	9,534	753	25	0	0.02	5	0.17	562	0.78
50%-ile	98.8%	11,019	1,228	39	3	0.04	6	0.26	847	0.87
75%-ile	98.9%	12,745	1,887	57	66	0.09	6	0.38	1,302	0.96
90%-ile	99.1%	14,946	2,988	85	170	0.18	7	0.61	1,889	0.99
99%-ile	99.3%	27,464	7,834	265	423	0.51	7	1.65	3,600	0.99

[a] Recovery energy efficiency is defined as the total energy output in oil, processed NG, and NGL divided by the total energy inputs, i.e. NG, diesel, and electricity as process fuels, and the oil, processed NG, and NGL produced from the wells;

[b] Weighted by total output of energy products, i.e., oil, natural gas, and natural gas liquids;

[c] Without energy-based allocation applied. Shale oil in Bakken has a LHV of 6.4 mmBtu per bbl.

Table 30. Summary of energy use intensities associated with shale oil production from flaring wells in Bakken, 2006–2013, using energy allocation method, except as noted

	Recovery Energy Efficiency[a]	NG Use (Btu/mmBtu of oil)	Diesel Use (Btu/mmBtu of oil)	Electricity Use (Btu/mmBtu of oil)	Operational Flaring Intensity (SCF/mmBtu of oil)	Fugitive Intensity (SCF/mmBtu of oil)	GOR[c] (SCF/bbl of oil)	O/T Ratio
Weighted average	98.9%	10,208	1,369	42	86	6	1,122	0.88
1%-ile	96.7%	6,043	221	1	0	4	143	0.56
10%-ile	98.3%	8,071	464	13	2	5	414	0.72
25%-ile	98.6%	9,217	795	24	9	5	600	0.82
50%-ile	98.8%	10,814	1,299	39	47	6	878	0.91
75%-ile	99.0%	12,622	1,959	59	132	7	1,322	0.99
90%-ile	99.1%	14,899	3,122	90	224	7	1,925	0.99
99%-ile	99.3%	28,061	8,121	283	502	7	3,607	0.99

Table 31. Summary of energy use intensities associated with shale oil production from non-flared wells in Bakken, 2006–2013, using energy allocation method, except as noted

	Recovery Energy Efficiency[a]	NG Use (Btu/mmBtu of oil)	Diesel Use (Btu/mmBtu of oil)	Electricity Use (Btu/mmBtu of oil)	Fugitive Intensity (SCF/mmBtu of oil)	GOR[c] (SCF/bbl of oil)	O/T Ratio
Weighted average	98.8%	10,871	1,197	40	5	1,249	0.82
1%-ile	97.0%	6,552	221	3	3	0	0.50
10%-ile	98.3%	8,855	419	18	4	278	0.67
25%-ile	98.6%	9,924	691	26	5	499	0.74
50%-ile	98.8%	11,251	1,144	38	6	802	0.83
75%-ile	98.9%	12,894	1,784	55	6	1,273	0.89
90%-ile	99.0%	14,995	2,795	79	6	1,841	0.94
99%-ile	99.2%	26,522	7,166	227	7	3,579	0.99

Wide variations in energy use and production among the thousands of wells are observed. To account for the effect of this variability on the estimation of GHG emissions with GREET, we characterized probability distribution functions (PDFs) of the major parameters, using 184,400 well-month observations in Bakken from 2006 to 2013.

We employ EasyfitTM, a curve-fitting toolbox, to find the probability distribution type from a pool of 55 distributions, e.g. Normal distributions, Weibull distributions, Uniform distributions, etc., that best fits the observations for each parameter. With the energy-based allocation method, we applied the total energy output of the main product and co-products as the weighting factor to fit the distribution. The higher the value of the weighting factor corresponding to a sample value of the parameter, the higher the possibility that the parameter has the sample value in the PDF to be fitted for the parameter. The toolbox uses one of the four well-known methods to estimate distribution parameters on the basis of available sample data: maximum likelihood estimates; least squares estimates; method of moments; and method of L-moments. The toolbox calculates the goodness-of-fit statistics, including the Kolmogorov Smirnov statistic, the Anderson Darling Statistic, and the chi-squared statistic, for each of the fitted distributions. Then the toolbox ranks the distributions on the basis of the goodness-of-fit statistics. We then selected the distribution with the highest rank, primarily based on the Kolmogorov Smirnov statistic.

Table 32 summarizes the PDFs of process fuel consumption intensities, flaring intensities, fugitive intensities, and water use for shale oil production in Bakken from 2006 to 2013.

Table 32. Probability distribution functions of key parameters for shale oil production in Bakken, 2006–2013

Parameter	PDF Type	PDF Parameter		
NG use, mmBtu/mmBtu	Lognormal	Mu	Sigma	
		-4.5952	0.24985	
Diesel use, mmBtu/mmBtu	Lognormal	Mu	Sigma	
		-6.8875	0.72035	
Electricity use, mmBtu/mmBtu	Gamma	Alpha	Beta	Gamma
		1.8796	0.000021795	0
Operational flaring intensity, scf/mmBtu	Weibull	Alpha	Beta	Gamma
		0.72097	70.81	0
Flaring efficiency	Weibull	Alpha	Beta	Gamma
		2426000000	7805000000	-7805000000
Fugitive intensity, scf/mmBtu	Normal	Mu	Sigma	
		5.7775	0.78279	
Water use, gal/gal of oil	Lognormal	Mu	Sigma	
		-1.7857	0.76465	

4.2 Well-to-Wheels GHG Emissions of Petroleum Fuels Derived from Shale Oil in Bakken

We configured the GREET model to calculate the well-to-wheels (WTW) GHG emissions of petroleum fuels derived from shale oil in Bakken. For GHG emissions associated with shale oil recovery, we used parametric assumptions in Table 29. We estimated the CO_2 and CH_4 emissions from gas flaring and fugitives, as shown in Table 33, based on the chemical compositions of the gas, as shown in Table 5.

For GHG emissions associated with refining of shale oil, we applied the regression formula we developed for estimating the overall refinery energy efficiency as well as the relative refinery energy requirements for specific petroleum products [51], using the API gravity, which is about 42, and the sulfur content, which is assumed 0.2% [52], of the shale oil in Bakken. It is noted that we constrained the upper limit for the API gravity in the regression formula to 39, which was the highest API observation that we sampled for developing the regression formula due to lack of information on the effect of higher API gravity than 39 on US refinery energy efficiencies [51]. Table 34 and Table 35 summarize the WTW GHG emissions and water consumption of gasoline, diesel, and jet fuels produced from shale oil in Bakken.

Table 33. CO_2 and CH_4 emissions from gas flaring and fugitives associated with shale oil production in Bakken

	CO_2, g/mmBtu	CH_4, g/mmBtu
Flaring	5,354	5
Fugitive	298	60
Total	5,652	65

Table 34. WTW GHG emissions, in g CO_2e/MJ, of gasoline, diesel, and jet fuels produced from shale oil in Bakken. WTR = Well-to-refinery gate; WTP = well-to-pump; PTW = pump-to-wheels.

	WTR[a]	WTP[b]	PTW[c]	WTW
Gasoline blendstock	8.8	21.4	73.2	94.6
Diesel	10.2	17.6	75.6	93.2
Jet	10.3	13.7	72.9	86.6

a: Well-to-refinery gate;
b: Well-to-pump;
c: Pump-to-wheels.

Table 35. WTW water consumption, in gallons/mmBtu, of gasoline, diesel, and jet fuels produced from shale oil in Bakken. WTR = Well-to-refinery gate; WTP = well-to-pump; PTW = pump-to-wheels.

	WTR[a]	WTP[b]	PTW[c]	WTW
Gasoline blendstock	4.8	21.4	0.0	21.4
Diesel	5.6	8.1	0.0	8.1
Jet	5.7	23.7	0.0	23.7

a: Well-to-refinery gate;
b: Well-to-pump;
c: Pump-to-wheels.

5 CONCLUSIONS

Production-weighted average energy intensities for natural gas, diesel, and electricity consumption are approximately 13,200, 1,800, and 50 Btu/mmBtu, respectively.

Total energy consumption in the Bakken, including energy consumed for non-productive purposes, is dominated by flaring. On average, over all years of interest, about 5–15% of the energy content of the crude oil produced in the Bakken is flared. For flaring wells, the production-weighted average flaring rate of ~500 scf/bbl in recent years equals about 14% of the energy content of the crude oil, or 140,000 Btu/mmBtu.

The modeled flaring efficiency in the Bakken is high, above 99.5% on a volume-weighted basis. Some flares are inefficient because of the combustion regime encountered with low gas flow rates and high cross-wind velocity, but these wells amount to a small volume of the gas flared and therefore do not materially affect the volume-weighted flaring efficiency.

Bakken wells produce a significant amount of co-product energy along with the reported crude + condensate production. In 2013, co-production of natural gas (net of on-site use) equaled some 50,000 Btu/mmBtu, while co-production of NGLs was approximately 140,000 Btu/mmBtu.

Resulting GREET-derived WTR GHG intensities range from 8.8 to 10.3 g CO_2eq./MJ LHV of fuel produced, depending on the fuel modeled.

6 REFERENCES

1. NDDMR, *Well-level production statistics: `all_prod' data series*, 2014, North Dakota Department of Mineral Resources.

2. NDDMR, *Well-level characteristics: `wellmaster' data series*, 2014, North Dakota Department of Mineral Resources.

3. ARB, *Carbon Intensity Lookup Table for Crude Oil Production and Transport*, 2014, California Air Resources Board: http://www.arb.ca.gov/fuels/lcfs/lcfs_meetings/111314handout1_crudeoil.pdf.

4. U.S. Department of State, *Keystone XL - Final supplemental EIS. Appendix U: Lifecycle Greenhouse Gas Emissions of Petroleum Products from WCSB Oil Sands Crudes Compared with Reference Crudes*, 2014, Department of State: http://keystonepipeline-xl.state.gov/documents/organization/221247.pdf.

5. IHS, *Comparing GHG Intensity of the Oil Sands and the Average US Crude Oil*, 2014, IHS Energy.

6. IHS, *Appendix to IHS Special Report: Comparing GHG Intensity of the Oil Sands and the Average US Crude Oil*, 2014, IHS Energy.

7. Schneising, O., et al., *Remote sensing of fugitive methane emissions from oil and gas production in North American tight geologic formations.* Earth's Future, 2014. **2**: pp. 548–558.

8. Kort, E.A., et al., *Four corners: The largest US methane anomaly viewed from space.* Geophysical Research Letters, 2014. **41**(19): p. 2014GL061503.

9. Caulton, D.R., et al., *Methane destruction efficiency of natural gas flares associated with shale formation wells.* Environmental Science & Technology, 2014. **48**: pp. 9548–9554.

10. NDDMR, *Well-level well-test and geologic test data: `geoprodtest' data series*, 2014, North Dakota Department of Mineral Resources.

11. NDDMR, *Well-level stimulation, workover dataset: `geostimulations' data series*, 2014, North Dakota Department of Mineral Resources.

12. Mitchell, R.F., and S.Z. Miska, *Fundamentals of drilling engineering*, 2011, Richardson, TX: Society of Petroleum Engineers.

13. FracFocus, *FracFocus Chemical Disclosure Registry*, 2014: http://www.fracfocus.org.

14. Ross, R., *Efficient fracture stimulation: Advances in Technology Panel*, in *Williston Basin Petroleum Conference*, Bismarck, ND, 2012.

15. Theloy, C., and S.A. Sonnenberg, *Factors influencing productivity in the Bakken play, Williston Basin*, in *AAPG Annual Convention and Exhibition*, Long Beach, CA, 2012.

16. The Engineering Toolbox, *Fuel gases - heating values*, 2014.

17. McNally, M.S., and A.R. Brandt, *The productivity and potential future recovery of the Bakken formation of North Dakota*. Journal of Unconventional Oil and Gas Resources, 2015. **11**: pp. 11–18. DOI: 10.1016/j.juogr.2015.04.002

18. McNally, S., *A characterization of the productivity, recovery, and future oil production potential of the Bakken formation of North Dakota*, MS Thesis, Department of Energy Resources Engineering, Stanford University, Palo Alto, CA, 2014.

19. Siegel, H., *Bakken well depths now reaching 27,000+ feet*, 2014 [cited Jan. 15, 2015]: http://www.dtcenergygroup.com/bakken-well-depths-now-reaching-27000-feet/.

20. Isbell, M., et al., *Drilling optimization approach improves drilling efficiencies in the Bakken field*, in *SPE Annual Technical Conference and Exhibition*, Amsterdam, 2014, SPE-170610-MS.

21. Scott, G., and L.M. Smith, *Successful application of innovative reaming and completion technology in Williston Basin wells*, in *SPE Production and Operations Symposium*, Oklahoma City, 2013, SPE-164508-MS.

22. Bassarath, W.D., and C.A. Manranuk, *Application of targeted bit speed (TBS) technology to optimize Bakken shale drilling*, in *SPE/IADC Drilling Conference*, Amsterdam, 2013, SPE-163406-MS.

23. Han, G., et al., *Practical directional drilling techniques and MWD technology in Bakken and Upper Three Forks formation in Williston Basin North Dakota to improve efficiency of drilling and well productivity*, in *SPE Unconventional Gas Conference and Exhibition*, Muscat, Oman, 2013, SPE 163957-MS.

24. Djurisic, A., et al., *Williston Basin - A history of continuous performance improvements drilling through the "Bakken*," in *IADC/SPE Drilling Conference and Exhibition*, New Orleans, 2010, SPE 128720-MS.

25. Haliburton, *Haliburton MegaForce drill bits set new performance benchmark in hard/abrasive proving grounds*, 2014: http://www.halliburton.com/public/sdbs/sdbs_contents/Case_Histories/web/H011057.pdf.

26. Kammerzell, J., *New downhole drilling slurry saves customers money*, 2012 [cited Jan. 15, 2015]: http://www.pro1industrial.com/rigzone-article-101912-new-downhole-drilling-slurry-saves-customers-money/.

27. Newpark Drilling Fluids, *Evolution Brine System*, 2013.

28. O'Sullivan, F., and S. Paltsev, *Shale gas production: Potential versus actual greenhouse gas emissions.* Environmental Research Letters, 2012. **7:** p. 044030**.**

29. Allen, D.T., et al., *Measurements of methane emissions at natural gas production sites in the United States.* Proceedings of the National Academy of Sciences, 2013. **110**(44): pp. 17768–17773.

30. Brandt, A.R., et al., *Methane Leaks from North American Natural Gas Systems.* Science, 2014. **343**: pp. 733–735.

31. EDF, *Co-producing wells as a major source of methane emissions: A review of recent analyses*, 2014, Washington, DC.: Environmental Defense Fund.

32. Stirm, B., et al., *Efficiency of natural gas flares associated with shale formation wells*, in *American Geophysical Union Fall Meeting*, San Francisco, 2012.

33. El-Houjeiri, H., et al., *Oil Production Greenhouse Gas Emissions Estimator. OPGEE version 1.1 draft D: Computer program*, 2014, Palo Alto, CA: Department of Energy Resources Engineering, Stanford University.

34. Vafi, K., and A.R. Brandt, *GHGFrac: An open source model for estimating greenhouse gas emissions from hydraulic fracturing.* In preparation, 2015.

35. Azar, J.J., and G. Robello, *Drilling Engineering*, 2007, Tulsa, OK: PennWell Publishers.

36. Slagle, K.A., *Rheological design of cementing operations.* Journal of Petroleum Technology, 1962, **1962**(March): pp. 323–328.

37. Kurtoglu, B., *Integrated Reservoir Characterization and Modeling in Support of Enhanced Oil Recovery for Bakken*, Ph.D. Thesis, Department of Petroleum Engineering, Colorado School of Mines, Golden, CO, 2013.

38. Harju, J., *Overview of the EERC's Bakken CO_2 EOR Research Programs*, in *8th Annual Wyoming CO_2 Conference*, Casper, WY, 2014.

39. Boyer, R., et al., *Production array logs in Bakken horizontal shale play reveal unique performance based on completion technique*, in *SPE Annual Technical Conference and Exhibition*, San Antonio, TX, 2012, SPE-160160-MS.

40. Tabatabaei, M., D. Mack, and R. Daniels, *Evaluating the performance of hydraulically fractured horizontal wells in the Bakken shale play*, in *SPE Rocky Mountain Petroleum Technology Conference*, Denver, CO, 2009, SPE-122570-MS.

41. Tran, T., *Bakken shale oil production trends*, MS Thesis, Department of Petroleum Engineering, Texas A&M University, College Station, TX, 2011.

42. Yu, W., and K. Sepehrnoori, *Optimization of well spacing for Bakken tight oil reservoirs*, in *SPE/AAPG/SEG Unconventional Resources Technology Conference*, Denver, CO, 2014, SPE-2014-1922108-MS.

43. NDPC and M.C. Turner, *The North Dakota Petroleum Council Study on Bakken Crude Properties*, 2014, North Dakota Petroleum Council.

44. Bakken Shale, *BakkenShale.Com, tags: Hess Tioga Plant*. 2014 1/31/2015]: http://bakkenshale.com/tag/hess-tioga-plant/.

45. Wood Group Mustang. *Mustang awarded detailed design by Hess Corporation for Tioga gas plant expansion in North Dakota*, 2011 [cited Jan. 21, 2015]: http://www.mustangeng.com/NewsandIndustryEvents/PressReleases/Pages/MustanggHessTiogaExpansionProject.aspx.

46. Yeh, S., et al., *Land use greenhouse gas emissions from conventional oil production and oil sands*. Environmental Science & Technology, 2010. **44**(22): pp. 8766–8772.

47. Bokowy, T., *Shale oil logistics: Bakken crude routes and logistics*, 2014, Sandpoint, ID: Cost&Capital.

48. NDPA, *North Dakota Pipeline Authority: NDPA website datafile*, 2014, North Dakota Pipeline Authority.

49. NDPA, *North Dakota Pipeline Authority: Monthly Update*, 2007–2014, North Dakota Pipeline Authority.

50. DistanceCities, *Distances between cities*, 2015 [cited Jan. 15, 2015]: http://www.distance-cities.com/.